Understanding complex volcanic hydrosystems using a multi-tracer approach

Pierre Nevers, Hélène Celle, Cyril Aumar, Virginie Vergnaud, Barbara Yvard, Gilles Mailhot

Science of the Total Environment 964 (2025) 178421

Contents lists available at ScienceDirect

Science of the Total Environment

journal homepage: www.elsevier.com/locate/scitotenv

Understanding complex volcanic hydrosystems using a multi-tracer approach

Pierre Nevers [a,*], Hélène Celle [a], Cyril Aumar [a,b], Virginie Vergnaud [c], Barbara Yvard [c], Gilles Mailhot [d]

[a] Université de Franche-Comté, CNRS, CHRONO-E (UMR 6249), F-25000 Besançon, France
[b] Université Clermont Auvergne, CNRS, IRD, OPGC, Laboratoire Magmas et Volcans, F-63000 Clermont-Ferrand, France
[c] Univ Rennes, OSUR, UMR 3343, Plateforme Condate Eau, F–35000 Rennes, France
[d] CNRS, SIGMA Clermont, Institut de Chimie de Clermont-Ferrand, Université Clermont Auvergne, F-63000 Clermont-Ferrand, France

HIGHLIGHTS

- The study focuses on continental volcanic hydrosystems still poorly investigated.
- This study is based on a multicriteria analysis of geology, hydrodynamics and chemical tracers, highlighting water residence time as an essential element for better understanding the Volvic hydrosystem functioning.
- This study revealed bi-modal recharge pattern, leading to a significant enhancement of the hydrogeological conceptual model of the Volvic watershed.
- Understanding the functioning of Volvic hydrosystem is essential for assessing the sustainability of its water resources within time (past and future).

GRAPHICAL ABSTRACT

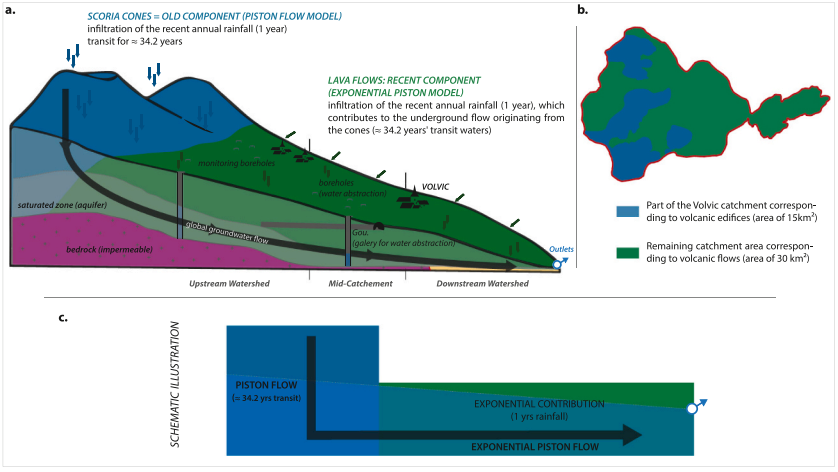

ARTICLE INFO

Editor: Dan Lapworth

Keywords:
Hydrochemistry
Chlorofluorocarbons (CFCs)
Tritium
Mean residence time
Volcanic aquifers
Climate change

ABSTRACT

Climate change affects groundwater availability and residence times, necessitating a thorough understanding of aquifer characteristics to define sustainable yields, particularly in regions where water is heavily exploited. This study focuses on the Volvic volcanic aquifer (Chaîne des Puys, France), where groundwater recharge has decreased due to climate change, raising concerns about water use sustainability. To address these challenges, this work proposes a multi-tracer approach, based on hydrogeological monitoring, including the estimation of groundwater ages, major elements chemistry and water stable isotopes to better characterise this resource decrease and more peculiarly its origin and its impact on the environment that has never been addressed. Relative fractions of ancient and modern water contributions (up to 20 %) to the aquifer have been thus estimated as well as the apparent ages of groundwaters (34 years). We highlight the complementarity of tracers

* Corresponding author.
E-mail address: pierre.nevers@univ-fcomte.fr (P. Nevers).

https://doi.org/10.1016/j.scitotenv.2025.178421
Received 28 June 2024; Received in revised form 7 December 2024; Accepted 6 January 2025
Available online 24 January 2025

used, allowing a better definition of recharge sources and transit times of groundwaters within the aquifer. These results led to the proposal of a hydrogeological conceptual model, highlighting a bi-modal recharge, distinguishing between a long-term recharge upon 30 years, supplemented by a recent component (≃ 1 year) related to annual precipitation. This study provides valuable information on groundwater circulation and the response of volcanic aquifers systems to climate change, while highlighting the importance of assessing residence times. By addressing the challenges posed by systems with contrasting permeability and recharge gradients, it improves understanding of volcanic hydrology and provides a basis for the development of (numerical) hydrological models to assess the impacts of global change.

1. Introduction

In the 21st century, the global hydrological cycle and catchments are likely to face significant and amplified changes due to a variety of factors, including climate change, land use/land cover change, population growth and urbanisation, and a consequent increase in water demand (Rockström and Steffen, 2009; Prudhomme et al., 2014; Cosgrove and Loucks, 2015; Murray et al., 2012; Cotterman et al., 2018). The Intergovernmental Panel on Climate Change (IPCC), in its sixth assessment report (IPCC: Climate Change, 2021) states thus that the Earth's surface temperature increased by an average of 1.59 °C for the period 2011–2020 and may increase up to 3 °C till 2060 (SSP5–8.5 scenario). This increase of air temperature results in modifications within the hydrological cycle (Parajuli, 2010; Wigley and Raper, 2001; Nearing et al., 2005; Githui et al., 2009; Dayon et al., 2018; Strohmenger et al., 2022) such as an increase of the frequency and intensity of extreme precipitation events or droughts, and a decrease of the recharge rate by effective rainfall of surface and groundwater (Arnell, 2011). As a result, river flows (Sauquet et al., 2021; Labrousse et al., 2022; Labbe et al., 2023; Shinhu et al., 2023) and groundwater levels (Ascott et al., 2022; Baulon, 2023; Labbe et al., 2023; Jascheko et al., 2024) around the world are falling, creating or increasing tensions over water resources that can degenerate into real conflicts of use. These tensions do not spare volcanic aquifers (Waibel et al., 2013; Uriostegui et al., 2016; Magi et al., 2019), which remain relatively poorly understood, particularly in continental areas. This is mainly due to their high dependence to the geological settings that is different from one site to another even if some attempts to produce a generic model has been achieved for andesitic island aquifers (Baud, 2024).

The Volvic volcanic aquifer is an excellent example of conflicting uses in continental volcanic zones. In fact, the volcanic formations of the Chaîne des Puys constitutes one of the main regional resources and have long been considered as the water tower of France considering the heavy rainfall (up to 1.5 m over Puy de Dôme – Canellas et al., 2014) that waters it. This aquifer provides water for domestic, agricultural and industrial uses (including bottling) and faces a hard decrease of its natural discharge since the 1980's, with an amplification for the last decade. The question is whether this decrease is solely due to a diminution in recharge or an increase in water abstraction. To solve this problem, a compilation of previous studies (Michel, 1957; Aubignat, 1973; Belkessa, 1977; Barbaud, 1983; Fournier, 1983; Bouchet, 1987; Belin et al., 1988; Gaubi, 1990; Joux, 2002; Livet et al., 2000; Josnin et al., 2007; Loock et al., 2008; Bertrand, 2009; Rouquet, 2012; Aumar, 2022) giving the main geological features and the hydraulic parameters (porosity and permeability) has been gathered with investigations on transit time through hydrochemical data, tritium and CFCs-SF_6measurements.

CFCs are widely used to date young groundwater, i.e., >50 years (Oster et al., 1996; Cook and Solomon, 1997; Busenberg and Plummer, 2000; Darling et al., 2012). Their application is valuable for estimating groundwater residence times, identifying mixing processes and understanding recharge patterns (Oster et al., 1996; Busenberg and Plummer, 2000; Gooddy et al., 2006; Gil-Márquez et al., 2020; Ranchoux et al., 2021; Okofo et al., 2022). However, there are limitations to their use, such as contamination by local sources, degradation under reducing conditions, and complex processes in the unsaturated zone (Heaton and Vogel, 1981; Cook et al., 1995; Gooddy et al., 2006; Cook et al., 2006; Gourcy et al., 2009) that can alter CFC concentrations, introducing temporal discrepancies between apparent and real water age. To reduce these ambiguities, CFCs are often combined with other tracers, such as SF_6 or tritium, providing a robust multi-tracer approach suitable for complex mixing scenarios (Han et al., 2007; Gourcy et al., 2009; Okofo et al., 2022).

In a volcanic environment such as Volvic, using SF_6 alone is not appropriate due to geogenic production of this element (Busenberg and Plummer, 2000; Koh et al., 2007; Gourcy et al., 2009). The combination of tritium (to CFCs) can provide information because as a solute tracer it moves by advection with infiltrating water, whereas gas tracers include advection and diffusion (Stadler et al., 2008). Despite their limitations, CFCs remain essential tools for studying groundwater recharge and circulation dynamics, especially when integrated into a precise hydrogeological context and associated with advanced models (Busenberg and Plummer, 2000; Ma et al., 2019).

This approach provides thus new insight into circulations in continental volcanic areas and the impact of residence time on the reactivity of this type of aquifer to global change.

2. Materials and methods

2.1. Study area

2.1.1. Geography and climate

The Volvic watershed is located 15 km northwest from the city of Clermont-Ferrand (central part of France). It constitutes the north-eastern part of the Chaîne des Puys-Faille de Limagne tectonic site, UNESCO world heritage sites. Its surface is of 45 km^2 (hydrogeological limits), with a west-east preferential extension of 11 km and an altitude decreasing eastward from 1163 m.a.s.l to 380 m.a.s.l., where reaching the Limagne basin. Average rainfall on the Volvic watershed is of 776 mm, value stable over the last 30 years. Its spatial distribution is controlled by orographic precipitation and foehn effects: precipitation height decreases from 1000 mm on the summits to <600 mm in the eastern lower part of the watershed, within the Limagne basin (<400 m asl) (Joux, 2002; Rouquet, 2012). The average annual temperature is 9.4 °C for the 1959–2023 period (Meteo-France database).

The soil occupation is stable since 1992 and is composed of 52 % forest, 15 % farmland, 13 % grassland and 10 % urbanised areas. The remaining area includes arable land, industrial or commercial zones (SDES, IGN, European Environment Agency, 2019).

2.1.2. Geology

Volvic watershed is part of The Chaîne des Puys N-S volcanic alignment lying on fractured Variscan-age granitic substratum called “Plateau des Dômes”. The latter has been affected by different tectonic phases (Hercynian-Mid Carboniferous and Alpine-Miocene) resulting in a NE/SW fracturing and the subsidence of the Tertiary Limagne sedimentary basin 700 m below (Merle and Michon, 2001; Lustrino and Wilson, 2007). The Limagne fault separates the Plateau des Dômes from the Limagne basin. Numerous faults that cut across the Plateau des Dômes enhanced erosion (Pliocene), which create deep valleys (around

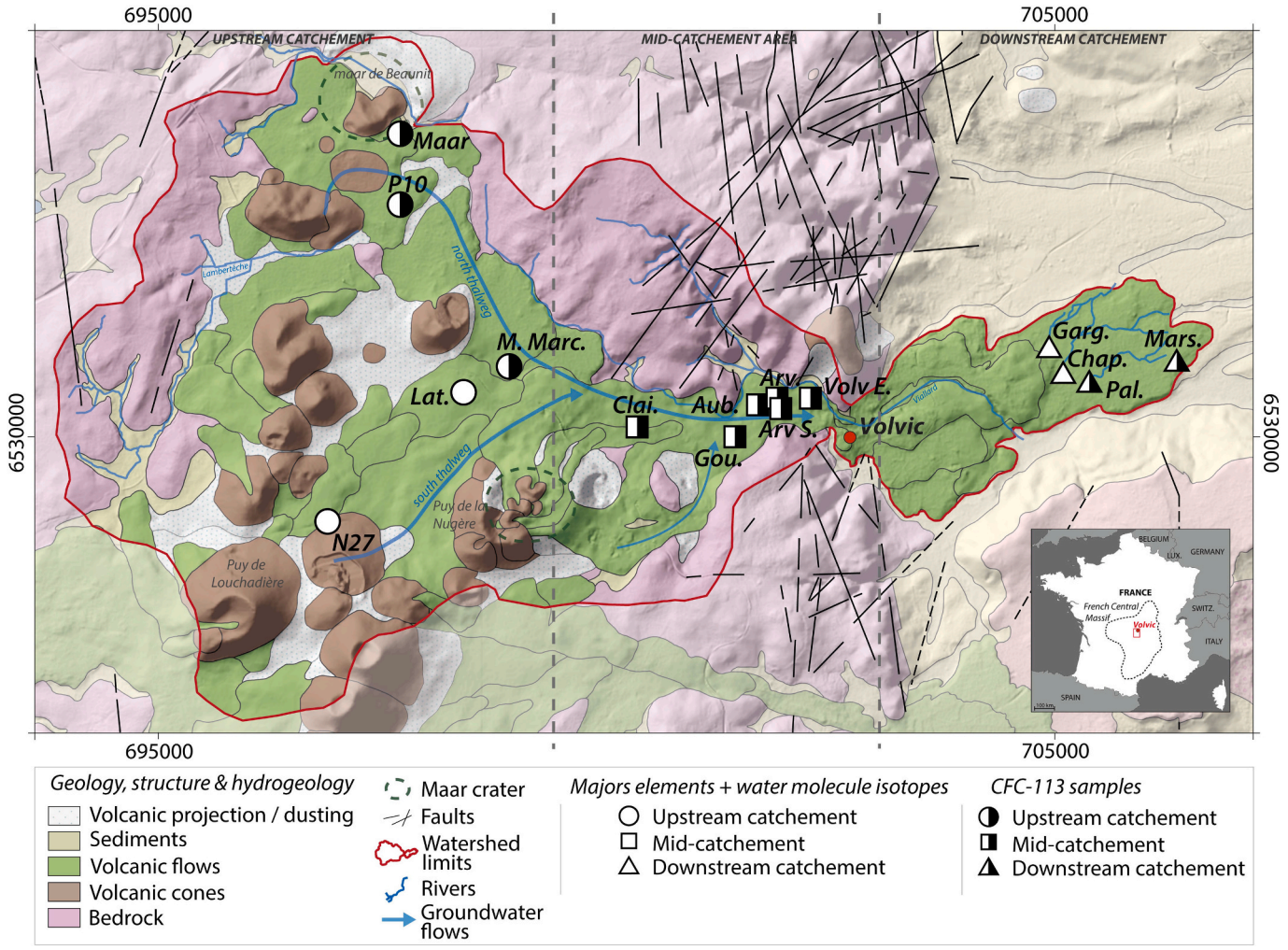

Fig. 1. Study site with geological, structural and hydrogeological information (from Boivin et al., 2017). Sampling points have been reported according their location within the basin.

200-400 m deep), mainly in an *E*-W direction (Michon and Merle, 2001; Merle et al., 2023). During the Quaternary, successive volcanic eruptions and issued lava flows from the Chaîne des Puys were channelled into these valleys (paleothalwegs), exhibiting different origins and petrology (Camus, 1975; Boivin et al., 2017; Harris et al., 2023), before reaching the Limagne plain. This regional volcanism is composed of various products issued from basic magmatism that produces rocks ranging from basalts to trachytes, including trachy-basalts and trachy-andesites (Janot and et, 2005; Rouquet et al., 2012; Boivin et al., 2017). This petrological diversity of the magmas and the environmental conditions during volcanic activity explain the multiplicity of volcanic structures: domes, scoria cones, maars, *pahoehoe* and *aa* lava flows (Loock et al., 2008; Boivin et al., 2017).

The studied catchment area is mainly occupied by volcanic formations (80 %) with 6 aa lava flows of variable extension and thickness, from 10 to 140 m (Figs. 1 and 2), which have gradually piled up in two main paleothalwegs that cut through the substratum in the southern and the northern part of the basin (Rouquet et al., 2012). In their eastern part, they spread in the sedimentary Limagne basin where they are thrown into relief inversion due to erosion processes (Fig. 2 c and d). In specific areas, such as the Nugère sector (scoria cones associated with maar structures), the thickness of the volcanic infill can reach >180 m (Boivin et al., 2017; Aumar et al., 2024). The granitic substratum (in pink on Figs. 1 and 2) constitutes the lower limit of the Volvic watershed which is delimited in its northern, western and south-western parts by the topography of the outcropping substratum whereas in its southern part, limits have been determined by geophysical investigation such as self-potential methods and Electrical Resistivity Tomography (Joux, 2002; CETE-BRGM, 2009; Aumar, 2022).

2.1.3. Hydrogeology

Hydrodynamic properties of the present formations vary according their nature, inducing complex runoff and groundwater flow at all scales (Custodio, 1985; Josnin et al., 2007; Bertrand, 2009; Lachassagne et al., 2014; Poncela et al., 2022). Scoria cones and maars (phreatomagmatism) are made of complex structure with scoria and pyroclastic deposits, that are highly porous and permeable: effective porosity of these formations is estimated between 30 and 45 % (Yokoyama and Takeuchi, 2009; Colombier et al., 2017; Aumar, 2022). Permeability of these material depends on the cohesion of volcano-clastic products and the connectivity of the pores they include. Lava flows can be highly heterogenous, depending on their petrology (Loock et al., 2008; Bertrand et al., 2010; Harris et al., 2023). Porosity and permeability, range from 5 % to 20 % and 10^{-3} to 10^{-5} m.s^{-1}, respectively, linked to their structure and degree of fracturing (Poncela et al., 2022). Moreover, when these flows are emplaced, their bases and flanks tend to cool more rapidly than the core, producing a scoriaceous level in contact with the surrounding rocks that may drain a part of the water circulation.

In Volvic and throughout the Chaîne des Puys, the hydrographic network is limited, rainwaters infiltrate preferentially through the

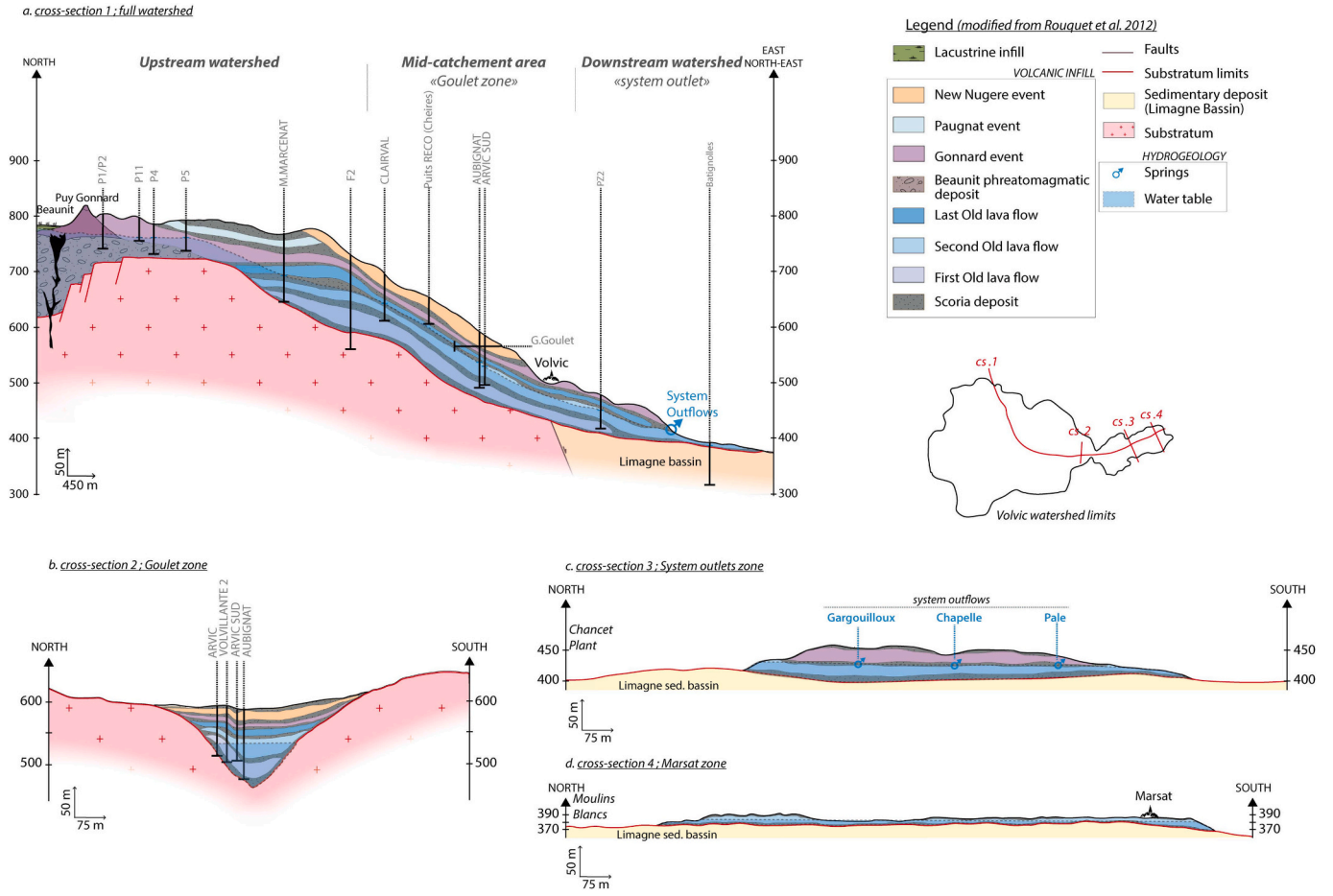

Fig. 2. Geology of the Volvic watershed a. North-East cross section (cs.1) b. c. d. North-South cross section from the mid-catchement (cs.2) to the downstream eastern part (cs.4) of the watershed.

infiltration of runoff or some small water courses at the contact between substratum and volcanic products (e.g., Lambertèche and Viallard, Fig: 1; Joux, 2002; Bertrand, 2009; Boivin et al., 2017) or directly thought the quaternary volcanic formations and/or the fissures (even if this vertical flow remains limited and can be disrupted by the massive structure of the flow cores (Barbaud, 1983; Celle-Jeanton et al., 2008; Bertrand et al., 2010). Infiltrated rainwater travel vertically through the volcanic pile, which can be up to 200 m thick in some paleovalleys, or even more in the case of scoria cones in the upstream part of the catchment. After percolation, meteoric waters reach the saturated zone established at the top of the substratum, made of impervious crystalline rocks and sedimentary formation in the Limagne basin; this latter is mostly considered as impervious even if some studies have recognized water reserves northward (Tweed et al., 2018). Groundwater then circulates at the interface between the bedrock and the volcanic formations or within the scoria layers at the bottom of each massive lava flows (Bertrand, 2009; Rouquet, 2012). Outlets of these volcanic hydrosystems emerge at the end of each lava flow, in the middle of catchments in the case of intra-volcanic springs (interface between two lava flows) or at the extreme downstream end of catchment in the case of infra-volcanic springs (Figs. 1 and 2).

The Volvic hydrosystem has been described as a superposition of semi-captive aquifer levels with preferential drainage axis, connected through vertical fractures and fissures of the compact lava layers (Joux, 2002). Its average thickness is about 40 to 50 m, mainly in the centre of the basin in the Goulet zone (Rouquet et al., 2012), tapering off upstream and downstream. The catchment area can be divided into three main areas based on hydrogeology and topography:

- Upstream catchment, mainly composed of scoria cones and 3 lava flows. Groundwater flow is divided into two main circulations following a northern and a southern axis (north and south thalweg, Fig. 1). The northern axis extends from the Maar de Beaunit (Fig. 1), which is included to the Volvic basin at its northern limit (Livet et al., 2000) and stores consequent volumes of water (several million m^3) with a slow renewal rate, to M.Marc. – Clai. sector. The southern axis extends from the Puy de Louchadière, Jumes, Coquille sector to join the northern axis between the sampling points M.Mar. and Clai.
- Mid-catchment area is characterized by the presence of 6 aa lava flows of variable extension and thickness, which have gradually piled up into a single narrow valley so-called “Goulet zone” (Van der Min, 1945; Barbaud, 1983; Joux, 2002; Rouquet et al., 2012).
- Downstream catchment is the lower part of the Volvic catchment and corresponds to the end of the lava flows (in relief inversion) in the Limagne plain (easter end of the watershed; Fig; 1 and 2). Three main emergences (Fig. 1and 2: Garg, Pal, Chap) emerge at a slope break corresponding to the end of a lava flow (Joux, 2002). A fourth spring (Mars, Figs. 1 and 2d) is identified at the extreme eastern end of the last volcanic flow. Other springs are probably located on the periphery of this front, but are of a low flow rate or are not permanent. These springs feed the hydrographic network of the Riom plain, towards the Limagne. The mean outflow from the Volvic catchment volcanic aquifer is estimated around 335 $L.s^{-1}$ for the year 2022 and was approx. About 450 $L.s^{-1}$ in 2002 (Joux, 2002).

The studied aquifer system displays high regulation capacity, the slow transit of groundwaters through formations means that climatic

Table 1
Location of the MeteoFrance network meteorological stations used in this study.

Name	Code MeteoFrance	Lat.	Long.	Elev. (mNGF)	Operating period
VOLVIC	63,470,001	45.8765	3.0508	472	1947 to 2018
SAYAT_SAPC	63,417,001	45.8396	3.0451	550	1993 to date
CLERMONT-FD	63,113,001	45.7868	3.1493	331	1923 to date
FONTAINE-DU-BER_SAPC	63,263,005	45.7995	2.9916	971	1930 to date
PLAUZAT_SAPC	63,282,001	45.6323	3.1336	503	1995 to date
ST-GENES-CHAMPE	63,346,001	45.4175	2.7236	1010	1951 to 2020
ST-GERVAIS-DAU	63,354,004	46.0326	2.8038	705	1964 to date

variations are regulated, resulting in moderate piezometric fluctuations and a high degree of consistency in the volcanic springs. This is associated with the buffering capacity of the scoria that constitute the aquifer reservoir (Josnin et al., 2007; Rouquet et al., 2012; Boivin et al., 2017). Fissure flows and scoriaceous sole, in contrast, exhibit high permeability, allowing rapid flows (Celle-Jeanton et al., 2008). Some previous studies have characterized the chemical composition broadly and mainly focused on the potential sources of contamination of aquifers levels by specific chemical constituents (Joux, 2002; Rouquet, 2012). A quite homogeneous chemical composition is highlighted due to a buffering by large volumes of waters within the system. Some evidence of higher contamination (anthropogenic inputs related to surface water infiltration), depending on the section of the catchment area considered, has however been showed due to rapid transfers associated with runoff infiltration at the contact between basement/lava flow (Joux, 2002; Rouquet, 2012).

2.2. Data, samples and analytical methods

2.2.1. Climatic data

Meteorological data (precipitations in mm, atmospheric temperatures in °C) were provided by the public data portal Meteo-France on the grid point (8 km^2) corresponding to the Volvic watershed (Lat, Long of the point: 45.8711,3.0064). For this grid point, data are available from 1959 for both rainfall and temperature. Meteorological data from the Sayat_sapc and Volvic stations were also used (Table 1 - https://publithe que.meteo.fr). Actual Evapotranspiration (AET) was computed following Oudin et al. (2005). RU has been set to 70 mm for water budget computations, on the basis of previous studies (Joux, 2002) and soil data obtained from INRAE datasets online (Le Bas, 2018; https://a groenvgeo.data.inra.fr/ geonetwork/srv/fre/catalog.search#/metadata/393d8106–4400-51 cd-9767 e8bbef2f73a6). Recharge was estimated using the ESPERE spreadsheet (Lanini et al., 2015).

Spatialization of the recharge presented in the results section (3.1) of this paper uses the meteorological stations of the Meteo-France network listed in Table 1.

2.2.2. Hydrodynamic data

Discharge is measured hourly at hydrometric stations operated and managed by the DREAL (https://www.hydro.eaufrance.fr/stationhydro). These stations are located at the three main outlets of the aquifer system: Garg, Chap and Pal. The Chap. source has been monitored since 1975, while the other two (Garg. and Pal.) are instrumented from 2010.

Groundwater level data (produced by water managers) used in this work correspond to the Clai. borehole, used for bottling (Fig. 1 and 2), which presents the longest (from 2002) and most representative (location in the centre of the watershed) record available for the catchment area. Clai. borehole (Lat. 45.869913; Long. 3.006409; Alt.: 701.96 mNGF) is 85 m deep and the average static level in 2022–2023 was −61.2 m (± 0.4 m) relative to the top of the structure.

It should be pointed out that the Volvic catchment area is subject to water abstraction for drinking water supply (since 1929) and for industrial purposes, including bottling (since 1965). The volumes abstracted (for all purposes) currently stand around 225 $L.s^{-1}$ (a relatively constant value since 2005), with seasonal variations linked to water needs and consumption. Abstraction data used in this work comes from historical monitoring carried out by the authorities responsible for each of the concerned resources and are therefore not publicly available.

2.2.3. Hydrochemical data

In situ measurements of water pH, and electrical conductivity (EC) were performed using PONSEL ODEON® Digital Handheld Instrumentation equipped with pH probe and a 4-electrode conductivity sensor (2 graphite, 2 platinum) with accuracies of 0.1 pH units and 1 % for pH and EC respectively. CTD-Diver probes (DI28x Series -vanEssen) are also used to measure electrical conductivity (with an accuracy of ±2 %) and temperature (± 0.1 °C) at high frequency (every hour) at the following locations: Maar, P10, M.Marc, Gou, Garg, Chap, Pal and Mars. The French National Geological Survey (BRGM) also provides EC and temperature measurements for points Lat. and N27 measured with OTT-CTD probes (Hydromet) with accuracies of ±1.5 % and ± 0.1 °C respectively.

The sampling includes a total of 43 water samples collected from 15 sites of the Volvic watershed during 3 field campaigns conducted in June 2022, October 2022 and February 2023 (Table 1, Fig. 1). Sampling locations are separated into 3 groups: upstream catchment (Maar, P10, M. Marc, Lat., N27), mid-catchment (Clai., Aub., Gou, Arv., Arv S., Volv E.), and downstream catchment (Garg., Chap., Pal., Mars.). Physical parameters, major elements and water stables isotopes ($\delta^{18}O$-$\delta^{2}H$) analysis were conducted for each of the 43 samples. Tritium (^{3}H), Chlorofluorocarbons (CFC) and Sulfur hexafluoride(SF_6) and dissolved noble gases analyses were conducted for samples collected during the October 2022 and February 2023 campaigns, the first campaign (June 2022) served as an exploratory campaign to assess the feasibility of CFC-SF_6 sampling. Tritium were analysed for 15 sampling points, representing 30 samples. Chlorofluorocarbons and dissolved gases analysed were done on sampling points selected regarding the feasibility of the sampling procedure, thus 10 (October 2022) and 11 (February 2023) sampling points were selected for sampling and the analysis of 21 samples in total.

From a hydrometeorological point of view, samples were taken in close conditions (no exceptionally distinct high and low water periods), the context of the year 2022 having been particular with little precipitation, periods of significant temperatures and relatively low flows (at the outlets) and low groundwater levels (Fig. 5). Thus, samples were collected during periods of slightly high water in Oct-2022 and low groundwater levels in Feb-2023 with limited amounts of precipitation.

For major ions analysis, samples were collected in polyethylene bottles and filtered through 0.22 μm pore size nylon filters before being stored under refrigerated conditions for determination of major element concentrations. All major dissolved elemental analyses were performed at Laboratoire Chrono-Environnement (UMR 6249), Université de Franche-Comté. Concentrations of major dissolved cations were determined using atomic absorption spectroscopy (AA 100 PerkinElmer) with detection limits of 0.5, 0.1, 0.01, and 0.1 mg L-1 for Ca^{2+}, Mg^{2+}, Na^{+}, and K^{+}. Concentrations of dissolved anions were determined using high-pressure ion chromatography (Dionex DX 100) with detection limits of 0.1, 0.1, and 0.05 mg L-1 for Cl^{-}, SO_4^{2-} and NO_3^{-}, PO_4^{3-}. HCO_3^{-} concentrations were determined with an accuracy of 1 % by acid titration (N/50 H_2SO_4) within 48 h after sampling. The dissolved silica concentration was analysed with a spectrophotometer (Spectroquant, Pharo 300, Merck) using a silica test kit (Merck) with an accuracy of 3 %. Only analyses with a charge balance lower than 10 % were considered.

Samples for water stable isotopes analysis were taken in 20 mL amber glasses bottles with hermetic cap, filled to the top with no headspace to avoid air entrapment and prevent isotopic fractionation.

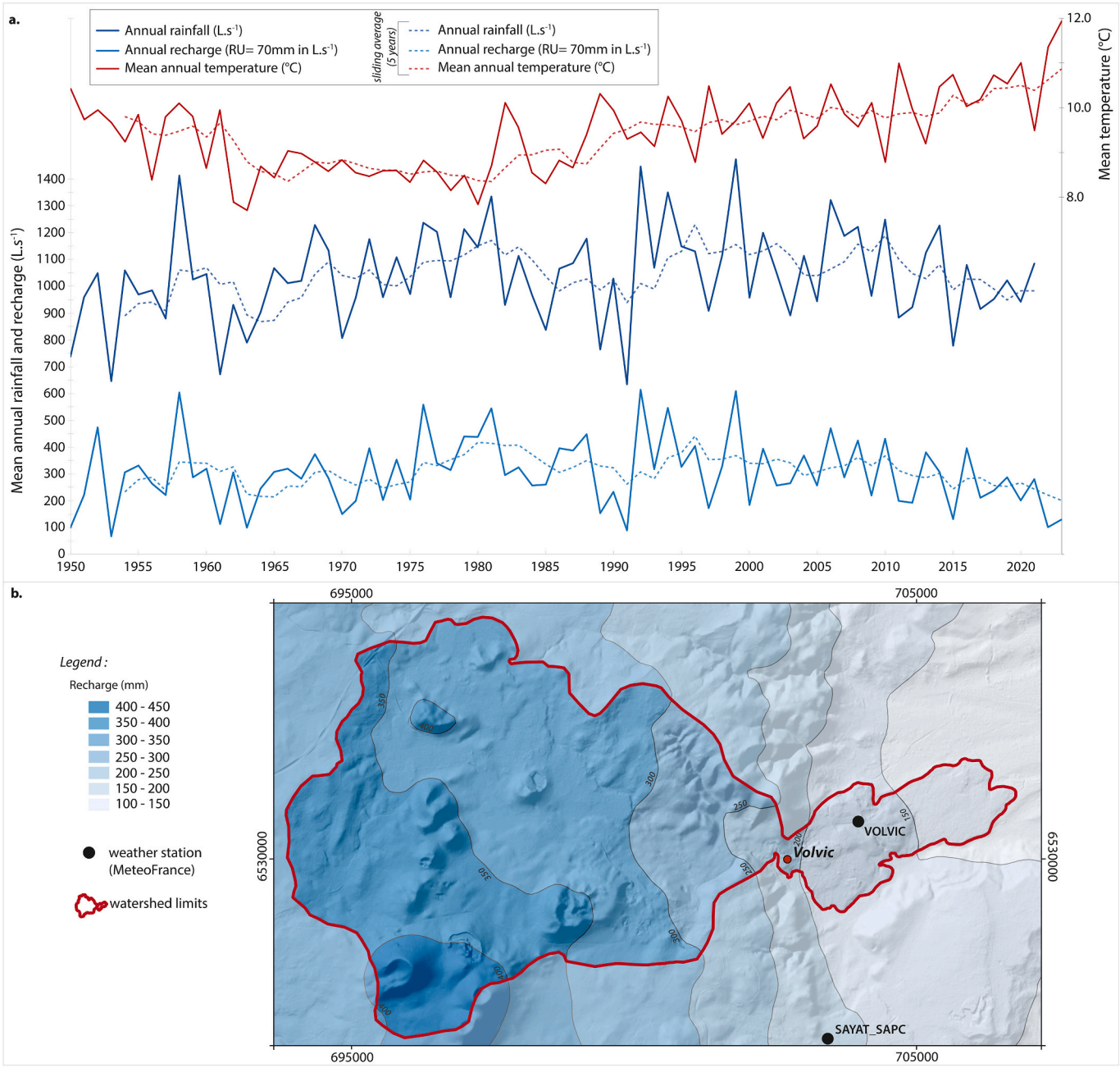

Fig. 3. : a; Evolution of the mean annual rainfall (mm), recharge (mm) and temperatures(°C) from 1950 to 2023 of the Volvic catchment area. Dashed lined correspond to 5 years sliding averages. b. recharge spatialization over the Volvic catchment for the period 2000–2021.

Rain samples were collected from a Palmex RS1 rain & snow sampler (evaporation free) installed at the M.Marc. point at elevation 761 mNGF. Water is collected in a 3 L plastic bottle and are then sampled using the same procedure described previously using 20 mL amber glasses bottles. Sampling for rainwaters has been done each month in 2022 from June to December (except August) and in March and May 2023. $\delta^{18}O$ and $\delta^{2}H$ measurements were performed at The Department of Hydrogeology of the University of Corsica, France (CNRS UMR 6134), using a liquid–-water stable isotope analyzer DLT-100 (Los Gatos Research) according to the analytical scheme recommended by the International Atomic Energy Agency (Penna et al., 2010). Values are presented in per mil units (‰) compared to Vienna Standard Mean Ocean Water standard (VSMOW). Quality of the isotopic analysis was checked using a standard deviation up to 0.1 ‰ for $\delta^{18}O$ and up to 1 ‰ for $\delta^{2}H$.

Water samples for tritium analysis were taken in 1 L PE bottles. Analyses were carried out at the laboratory Hydroisotop GmbH by Liquid Scintillation Spectrometry (LSC) after concentration with electrolysis. Measurements are given in tritium units (TU) with a double standard deviation (1 TU = 0.119 Bq. L-1). Results are relative to the date of measurement (no half-life correction).

2.2.4. *Chlorofluorocarbons (CFC-SF$_6$) and dissolved noble gases*

Water samples for CFCs (CFC-11, CFC-12 and CFC-113) and SF_6 were sampled in stainless steel ampoules (40 mL and 300 mL respectively) after washing through at least three volumes of the ampoule before closing it. No contact with air was allowed during sampling. Water for noble gas analyses was sampled in 500 mL glass bottles by overflushing. The bottles were submerged in flowing water, flushed, and capped without headspace. Sampling in wells equipped with pumps was carried out directly at the raw water tap closest to the wellhead (before

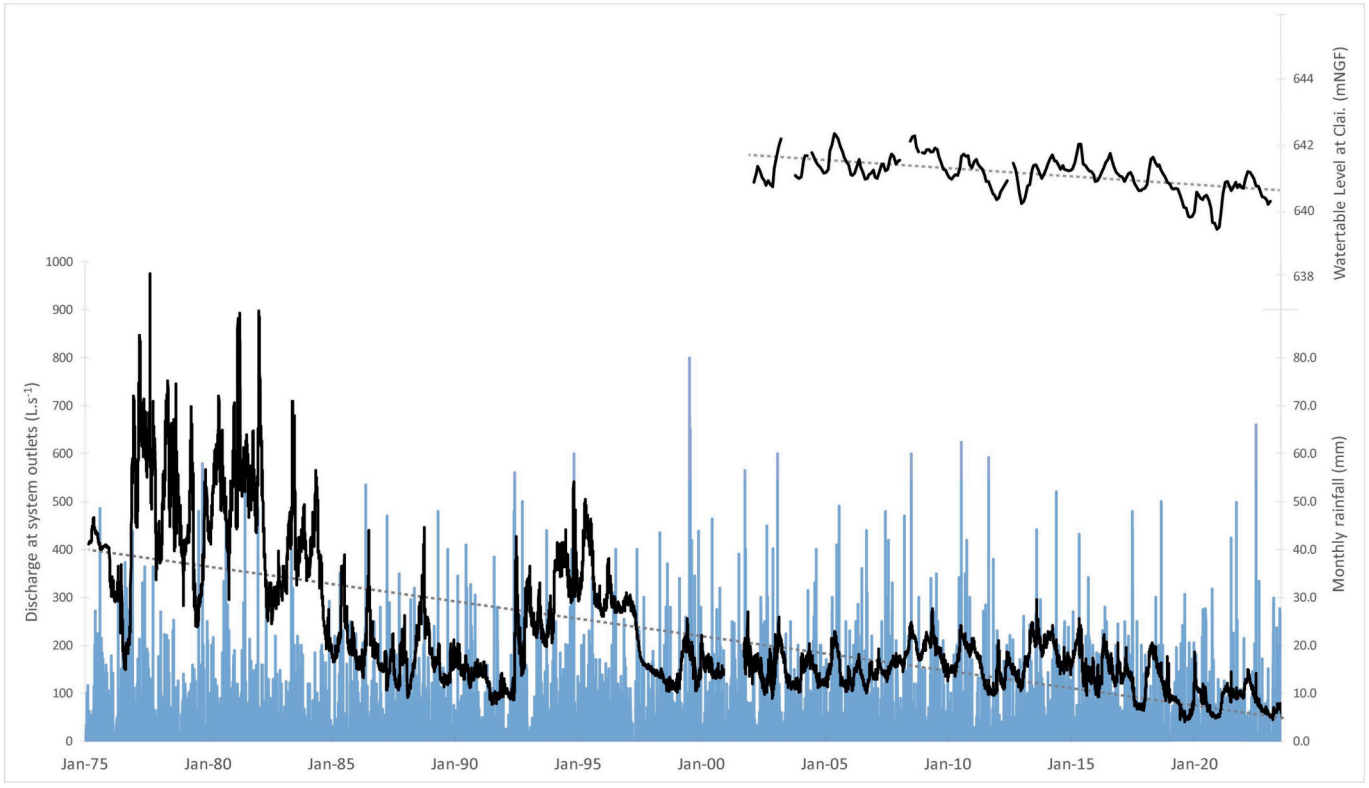

Fig. 4. : Monthly precipitation (mm) at Volvic weather station, monthly watertable level at Clai. (mNGF) and monthly discharge ($L.s^{-1}$) at the system's outlets from 1975 to 2023.

treatment or any storage tanks) to minimize the risk of contamination (pump running continuously during sampling). In boreholes, sampling was carried out using a submersible pump. Sampling is carried out after purging the well, once the physico-chemical parameters have stabilized, and at least after 20 min of pumping. In the case of springs, sampling was preferably carried out at the emergence point (where the flow rate is at its maximum) using a submersible pump. Low-flow pumping is maintained for at least 20 min. For each campaign analyses were performed at the CONDATE Eau Platform (OSUR, Rennes university, France) quickly after the sampling date.

Analyses for CFC-SF_6 were performed following the methodology described in Labasque et al. (2006) and Ayraud et al. (2008) using GC-ECD (Perkin- Elmer) with a Purge-and-trap (Busenberg and Plummer, 1992). Groundwater CFC and SF_6 concentrations were obtained by degassing water samples by N_2 stripping. Gases were trapped in a stainless-steel tube filled with HayeSep D, 60/80 Mesh (Restek) and maintained at −100 °C in an ethanol bath. After 6 (for CFCs) to 10 (for SF_6) min of pre-concentration, the trap is placed into boiling water to perform gas desorption. Gases were then injected into a gas chromatograph equipped with an electron capture detector (GC–ECD). Before starting any analysis, calibration with a standard (Greenland air calibrated by NOAA) is required. A system blank was also performed before each series of analyses. Analytical uncertainty is estimated to be 5 % for CFCs and SF_6. Age uncertainty varies as a function of concentration. Although the analytical uncertainty remains stable at 5 %, concentration variations may differ from period to period, leading to increased variability in ages, for example by 2 to 3 years between 1970 and 1990, and exceeding 10 years after 1995. In the case of CFC-113, the uncertainty in age is of the order of 1 year for a minimum concentration of 32.59 pptv and reaches 4 years for a maximum concentration of 85.26 pptv (although at +5 %, the latter exceeds the maximum value measured in the atmosphere). For an average concentration of 68.92 pptv, the uncertainty varies between 1 and 8 years, as this value can be read on both sides of the curve. After the atmospheric maximum, the slope of the curve curve decreases, thus increasing the uncertainty of the ages. Thus, the global uncertainty on age, including sampling, analysis, selection of the recharge temperature in Henry's law, and dispersion- adsorption effects, is estimated to ±10 %. Detection limits are 0.06 fmol/L for SF_6, 0.05 pmol/L for CFC-11, 0.02 pmol/L for CFC-12 and 0.015 pmol/L for CFC-113.

CFC and SF_6 concentrations were converted to atmospheric partial pressure (pptv) to be interpreted. Conversion was done using solubility functions for CFC-11, CFC-12, CFC-113 and SF_6 provided respectively by Warner and Weiss (1985), Bu and Warner (1995) and Bullister et al. (2002). Results obtained depend on recharge temperature, altitude and excess air (Darling et al., 2012).

Noble gases were analysed using a micro-gas chromatography system equipped with a thermal conductivity detector (GC 3000, SRA instrument). Gases were extracted by headspace extraction with a He (for Ne, Ar, N_2, O_2, CH_4 and CO_2 determination) or Ar (for He and H_2) carrier. The uncertainty is about 3 % for Ne measurements (water in equilibrium with air at 12 °C) and <2 % for Ar. This analysis allows calculation of excess air contribution from Ne concentration and determination of the Ne/Ar ratio for recharge temperature estimation (Chatton et al., 2016; Pérotin et al., 2021). Excess air calculations are used to correct SF_6 which can be strongly influenced by it, unlike CFC (Plummer et al., 2001; Vittecoq et al., 2007; Ayraud et al., 2008).

Apparent groundwater ages distribution was evaluated by using CFCs and ^3H data with the TracerLPM (version 1.1) workbook (Jurgens et al., 2012 – revised on march 2014), available from U.S. Geological Survey and following the IAEA "Use of Chlorofluorocarbons in Hydrology" guidelines (Plummer et al., 2006). TracerLPM provides solutions for the convolution integral for each of the LPMs (Lumped parameters Models) used in the present study: Four models were tested to determine the residence times for all samples: Piston Flow Model (PFM), Exponential Mixing Model (EMM), Binary Mixing Model (BMM) and the Exponential Piston Model (EPM).

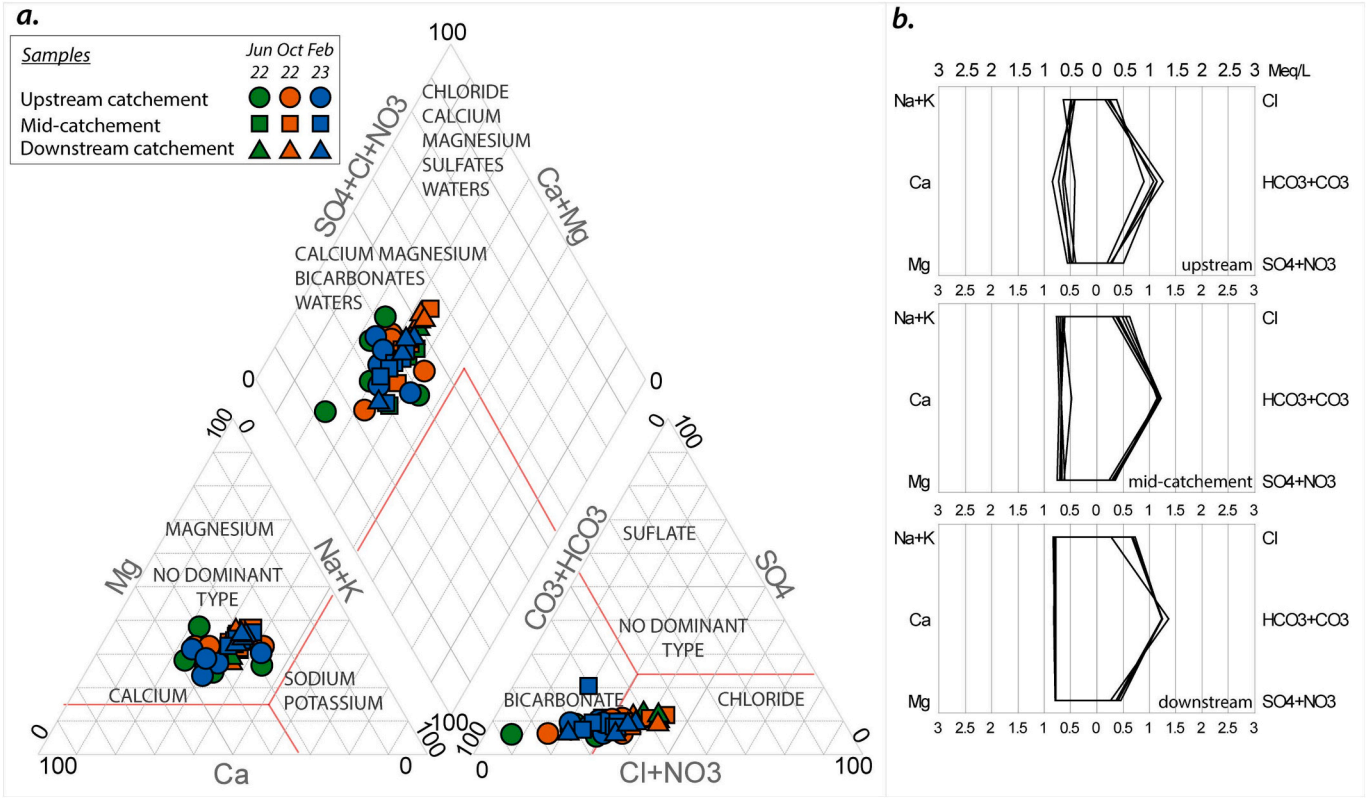

Fig. 5. : a. Piper diagram representing the chemical composition (Jun-2022, Oct-2022, Feb-2023) of waters sampled on the Volvic watershed (upstream, mid-catchment, downstream) b. Stiff diagram representing the facies of the different water group: upstream catchment, mid-catchment and downstream catchment waters during the three campaigns.

3. Results

3.1. Climatic features

Available databases (Meteo-France) provide 70 years of rainfall and temperature data for the Volvic catchment area, allowing thus to compute the recharge. There is no clear evolution in annual rainfall from 1950 to date and the mean annual rainfall is of 726 ± 120 mm (Fig. 3). Temperature shows a clear and gradual increase of 1.05 °C from the 1970s onwards (Fig. 3), in line with the conclusions of the IPCC in its sixth assessment report (IPCC: Climate Change, 2021). The average annual recharge over the period 1950–2023 stands at 227 ± 92 mm, representing 30 % of the total precipitation. Recharge, as temperature, decreases from the 1980s onwards.

Spatialisation of the recharge (Fig. 3b.) highlights a strong altitudinal gradient with values up to 2.1 times higher in the upper part of the catchment (> 800 mNGF) compared to the lower part (< 500 mNGF), supporting the findings of Joux (2002) and Bertrand (2009) that state that the upper part of the catchment of the Chaîne des Puys (> 800 mNGF) constitutes the major contribution to the volcanic aquifers. Estimated recharge gradient for the period 2000–2021 is around 42 mm/100 m.

3.2. Hydrodynamic

Discharge rates at the Volvic aquifer system's outlets have gradually decreased from 1975 (average of 457 $L.s^{-1}$ between 1975 and 1980) to 2023, with a mean value of 58 ± 11 $L.s^{-1}$ (Fig. 4). 2014–2015 marks the beginning of a more pronounced decline in discharge rates. From 2017 to the present day, low flow periods become more severe, with august 2019 showing the lowest values (40 $L.s^{-1}$) of the period. There is no real low-water period in 2021–2022, while in 2023 there is hardly any high-water period. Discharge monitoring implemented for the study period shows that discharge variations are nearly simultaneous to rainfall events.

Same tendency can be noticed for piezometric levels (Fig. 4) from 2002 (mean of 641.37 mNGF for 2002–2007) to 2023 (640.60 mNGF in average for 2018–2023). This represents a reduction of around 0.8 m in the water table level. Fluctuations in water levels generally follow a seasonal pattern between periods of high and low water, with a variation over a hydrogeological year usually around one metre, with a maximum variation of 1.8 m between 2018 and 2019. The amplitude of these variations remains very slight and represents a maximum of only 7.5 % of the water table thickness (with an average variation of 4.2 %, considering the 1 m amplitude). Groundwater level fluctuations are marked by a certain irregularity between seasons. The most notable are the severe low-water periods in 2019 and 2020, the absence of any significant high-water in 2020 and the absence of any low-water periods in 2022.

3.3. Hydrochemical characteristics of the groundwater system

3.3.1. Physicochemical parameters and major elements chemistry

Mean temperature of groundwaters for the three sampling campaigns is of 9.9 ± 1 °C close to the mean annual air temperature recorded at Volvic meteorological station (9.4 °C for the period 1959–2023) and the values given by the CTD-diver devices set up at points Maar, P10, M.Marc, Gou., Chap., Pal., et Garg. giving an annual average of 9.2 °C in groundwaters. pH is of 7 ± 0.3 close to neutral. Electrical conductivity (EC) ranges from 145 $\mu S.cm^{-1}$ (upstream) to 266 $\mu S.cm^{-1}$ (downstream) indicating poorly mineralised waters (mean: 206 ± 36 $\mu S.cm^{-1}$).

The chemical composition of groundwater is homogeneous and indicates a bicarbonate facies with no dominant cation (Fig. 5). Despite

Table 2
Physico-chemical parameters of groundwaters sampled in the Volvic watershed (for Garg. and Chap., measurements and sampling are carried out not directly at the outlet but several hundred metres after. Then values may thus differ slightly, particularly with regard to temperature).

Sample ID	Location	Altitude	Cond.	pH	T	Ca	K	Mg	Na	Si	HCO_3^-	F	Cl-	NO_3^-	SO_4^{2-}	PO_4^{3-}	δ^2H	±	$\delta^{18}O$	±
		(m .NGF)	*(µs/cm)*		*(°C)*	*(mg.L^{-1})*											*(‰)*		*(‰)*	
field campaign 1 - June 2022																				
Maar	**Upstream catchement**	781	189	7.5	9.6	14.9	3.6	8.6	7.4	13.6	105.6	0.2	4.1	0.8	5.8	n.a.	−57.7	0.27	−8.7	0.02
P10		803.2	195	7.3	9.8	18.3	4.1	6.3	7.5	15.5	77.7	0.1	6.2	24.1	5.1	n.a.	−52.9	0.25	−8.1	0.01
M.Marc		763.7	181	7.4	8.9	15.5	5.3	5.4	8.4	14.4	72.2	0.1	7.8	8.8	5.6	n.a.	−55.6	0.24	−8.4	0.05
Lat.		807	162	7.3	10.0	13.4	5.0	4.5	8.5	12.8	67.6	0.1	7.8	7.8	6.8	n.a.	−55.8	0.31	−8.5	0.04
N27		892.2	163	7.2	9.1	8.9	8.5	4.8	10.1	15.3	58.6	0.2	13.8	4.5	7.2	0.6	−57.2	0.22	−8.8	0.05
Clai.	**Mid-catchement**	708.8	184	7.3	11.8	10.2	7.5	7.0	10.7	15.6	78.0	0.3	10.8	6.1	7.0	0.8	−58.0	0.17	−8.8	0.02
Aub.		589.2	241	6.9	11.2	15.1	6.9	8.2	14.0	15.3	78.8	0.2	23.6	9.7	10.7	0.6	−56.7	0.61	−8.7	0.05
Arv.		584	208	7.1	11.0	14.2	6.5	7.3	11.2	14.8	79.5	0.2	14.0	7.8	8.1	0.6	−56.3	0.38	−8.4	0.01
Arv S.		585.2	216	7.1	11.4	14.3	6.6	7.5	11.9	14.9	76.8	0.2	17.4	9.0	9.3	0.6	−56.6	0.19	−8.6	0.03
Volv E.		579.3	222	7.0	11.0	14.6	6.9	7.8	12.8	15.0	77.3	0.2	19.5	9.3	9.7	0.6	−56.9	0.20	−8.5	0.01
Gou.		572.3	198	6.9	9.1	14.1	6.3	6.7	10.3	14.6	77.7	0.2	13.1	8.9	8.0	0.6	−56.0	0.13	−8.7	0.05
Chap.	**Down-stream catchement**	396.4	249	7.5	11.2	16.4	7.4	8.6	13.5	13.8	82.6	0.2	24.8	8.9	11.5	0.4	−56.2	0.26	−8.1	0.02
Pal.		394.7	266	6.9	10.1	17.6	7.1	9.0	15.3	15.1	80.4	0.2	27.0	12.7	13.4	0.5	−55.8	0.49	−8.1	0.01
Garg.		398.5	260	7.3	11.9	17.8	8.1	8.9	14.2	14.5	80.4	0.2	24.3	11.5	11.7	0.4	−57.1	0.22	−8.3	0.03
Mean			*210*	*7*	*10*	*15*	*6*	*7*	*11*	*15*	*78*	*0.2*	*15*	*9*	*9*	*1*	*−56*		*−8*	
Std. Dev.			*34*	*0.2*	*1*	*3*	*1*	*1*	*3*	*1*	*10*	*0.04*	*8*	*5*	*3*	*0.1*	*1.2*		*0.3*	
field campaign 2 - October 2022																				
Maar	**Upstream catchement**	781	145	6.7	10.0	12.3	3.5	5.5	7.6	14.8	46.5	0.1	7.1	14.0	6.1	n.a.	−54.6	0.33	−8.3	0.09
P10		803.2	181	6.2	10.2	16.7	4.1	7.4	7.7	14.9	59.2	0.1	6.0	26.2	5.1	n.a.	−53.1	0.63	−7.8	0.07
M.Marc		763.7	167	6.9	9.1	14.1	5.2	6.5	8.5	13.9	52.0	0.1	9.6	10.3	7.3	n.a.	−55.5	0.28	−8.5	0.06
Lat.		807	156	7.6	10.0	12.1	4.8	5.4	8.5	12.5	98.5	0.1	7.4	7.4	7.3	n.a.	−55.5	0.90	−8.4	0.13
N27		892.2	152	7.8	8.8	8.1	8.4	6.1	10.0	14.9	44.4	0.2	13.5	3.2	7.0	0.6	−57.4	0.65	−8.7	0.16
Clai.	**Mid-catchement**	708.8	172	7.2	9.6	9.3	7.4	8.4	11.0	14.9	59.5	0.2	10.4	6.2	6.8	0.8	−57.1	0.70	−8.8	0.06
Aub.		589.2	224	6.9	10.7	13.8	6.9	9.9	13.9	14.7	50.0	0.2	22.0	9.3	10.4	0.5	−56.3	0.45	−8.6	0.09
Arv.		584	200	6.9	10.8	13.2	6.5	8.8	11.4	14.2	61.2	0.2	14.7	8.3	8.7	0.6	−54.6	0.66	−7.9	0.06
Arv S.		585.2	211	7.0	10.7	13.3	6.8	9.2	12.4	14.5	62.0	0.2	17.3	8.7	9.3	0.5	−56.8	0.80	−8.7	0.13
Volv E.		579.3	212	7.0	10.7	13.1	6.7	9.2	12.8	14.6	66.7	0.2	19.5	9.1	9.7	0.6	−56.3	0.70	−8.6	0.05
Gou.		572.3	188	6.7	9.1	13.3	6.3	8.2	10.6	14.2	64.4	0.2	12.9	8.5	7.9	0.5	−56.2	0.29	−8.6	0.06
Chap.	**Down-stream catchement**	396.4	236	7.3	10.8	15.4	7.9	10.3	14.0	13.2	64.3	0.2	24.6	9.5	11.8	0.4	−57.1	0.33	−8.7	0.03
Pal.		394.7	246	6.6	10.2	15.7	7.3	10.5	15.1	14.6	64.2	0.2	24.7	12.4	12.5	0.5	−56.7	0.60	−8.6	0.14
Garg.		398.5	248	7.2	11.0	16.2	8.4	10.8	14.1	14.1	64.8	0.2	25.7	11.0	12.3	0.4	−57.3	0.50	−8.7	0.08
Mean			*195*	*7*	*10*	*13*	*6*	*8*	*11*	*14*	*61*	*0.2*	*15*	*10*	*9*	*1*	*−56*		*−8*	
Std. Dev.			*35*	*0.4*	*1*	*2*	*2*	*2*	*3*	*1*	*13*	*0.04*	*7*	*5*	*2*	*0.1*	*1.2*		*0.3*	
field campaign 3 - February 2023																				
Maar	**Upstream catchement**	781	148	7.0	8.7	12.6	3.1	5.1	7.7	14.7	58.1	n.a.	7.0	13.5	6.5	n.a.	−55.6	0.47	−8.5	0.06
P10		803.2	190	7.4	8.6	16.2	3.7	6.9	7.8	14.8	73.1	n.a.	5.7	25.5	5.5	n.a.	−54.3	0.29	−8.3	0.03
M.Marc		763.7	182	7.3	8.9	14.5	4.6	6.1	8.8	13.8	73.9	n.a.	9.7	10.2	7.7	n.a.	−55.7	0.16	−8.6	0.03
Lat.		807	156	7.4	–	12.1	4.2	4.9	8.6	12.5	67.1	0.2	7.2	6.6	7.7	n.a.	−55.0	0.39	−8.4	0.03
N27		892.2	173	7.5	–	8.3	7.1	5.6	10.1	14.5	60.8	0.2	13.7	3.0	7.5	0.9	−57.4	0.37	−8.8	0.00
Clai.	**Mid-catchement**	708.8	187	7.2	8.9	9.7	6.5	7.9	11.2	14.8	80.0	0.3	10.9	6.0	7.2	1.0	−57.1	0.52	−8.5	0.04
Aub.		589.2	247	6.9	10.0	14.2	6.3	9.3	13.8	14.6	82.9	0.2	21.9	8.9	10.9	0.9	−57.2	0.53	−8.7	0.06
Arv.		584	210	7.0	9.3	13.5	5.8	8.4	11.7	14.2	81.6	0.2	15.2	8.1	9.1	0.8	−57.0	0.71	−8.6	0.13
Arv S.		585.2	217	7.0	9.7	13.5	6.0	8.6	12.2	14.2	81.5	0.2	17.0	8.4	9.5	0.8	−56.0	0.40	−8.4	0.03
Volv E.		579.3	224	7.0	10.0	13.6	6.1	8.8	13.0	14.3	79.3	0.2	19.5	8.7	10.0	0.8	−56.6	0.14	−8.7	0.02
Gou.		572.3	204	7.0	9.0	13.6	5.7	7.8	10.9	14.0	82.3	0.2	13.2	8.2	8.5	0.8	−55.7	0.38	−8.4	0.06
Chap.	**Down-stream catchement**	396.4	258	7.6	4.2	16.1	7.2	9.9	14.1	13.3	83.4	0.2	24.6	12.1	12.5	0.8	−56.4	0.69	−8.3	0.06
Pal.		394.7	259	7.0	10.1	15.8	6.5	9.8	14.9	14.5	83.0	0.2	26.0	11.9	12.6	0.8	−56.6	0.75	−8.4	0.07
Garg.		398.5	259	7.3	7.8	16.1	7.1	9.8	13.9	14.1	81.3	n.a.	21.3	9.5	7.7	n.a.	−56.1	0.23	−8.5	0.03
Mars.		365	264	7.3	11.2	16.1	6.9	9.8	15.2	14.8	83.6	0.2	9.6	7.2	7.1	0.8	−56.8	0.18	−8.8	0.04
Mean			*212*	*7*	*9*	*14*	*6*	*8*	*12*	*14*	*77*	*0.2*	*15*	*10*	*9*	*1*	*−56*		*−9*	
Std. Dev.			*39*	*0.2*	*2*	*2*	*1*	*2*	*3*	*1*	*8*	*0.03*	*7*	*5*	*2*	*0.1*	*0.9*		*0.2*	
All campaigns - Mean			***206***	***7***	***9.9***	***14***	***6***	***8***	***11***	***14***	***72***	***0.2***	***15***	***10***	***9***	***1***	***−56***		***−8***	
Std. Dev.			***36***	***0.3***	***1***	***2***	***1***	***2***	***3***	***1***	***13***	***0.04***	***7***	***5***	***2***	***0.2***	***1.1***		***0.2***	
Rainwaters	***(mean)***																−45.9		−7.1	

Table 3
: Tritium (3H), CFC-SF6 and dissolved gases concentrations in groundwaters of the Volvic watershed

Sample ID	Location	^3H	±	SF_6		±	CFC-12		±	CFC-11		±	CFC-113	±	He	Ne	H_2	Ar	O_2	N_2	CH_4	CO_2	Number of valid tracers
		(TU)		*(pptv)*											*(mol.L^{-1})*								
field campaign 2 - October 2022																							
Maar	**Upstream catchement**	3.2	0.6	19.1	***E***	1.9	541.2		54.1	366.8	***E***	36.7	57.8	5.8	2.9E-09	7.9E-09	4.6E-10	1.5E-05	3.3E-05	5.3E-04	4.3E-09	3.6E-04	3
P10		3.2	0.6	21.9	***E***	2.2	562.8	***E***	56.3	389.6	***E***	39.0	68.0	6.8	3.5E-09	8.8E-09	3.8E-10	1.5E-05	2.9E-05	5.8E-04		3.5E-04	2
M.Marc		3.8	0.5	16.4	***E***	1.6	505.1		50.5	247.7		24.8	56.4	5.6	6.6E-09	7.8E-09	5.9E-10	1.5E-05	9.8E-05	5.7E-04	4.4E-09	2.6E-04	4
Lat.		3	0.5																				
N27		3.4	0.5																				
Clai.	**Mid-catchement**	4.1	0.6	16.4	***E***	1.6	516.9		51.7	253.6		25.4	69.3	6.9	6.6E-09	8.3E-09	4.7E-10	1.5E-05	1.3E-04	5.8E-04	1.0E-08	3.1E-04	4
Aub.		3.9	0.5	13.7	***E***	1.4	517.1		51.7	302.1	***E***	30.2	61.4	6.1	4.1E-08	7.5E-09		1.5E-05	1.9E-04	5.4E-04	6.8E-09	6.6E-04	3
Arv.		3.5	0.6	16.4	***E***	1.6	510.4		51.0	268.0		26.8	57.2	5.7	3.6E-08	7.3E-09		1.5E-05	2.2E-04	5.4E-04	4.7E-09	5.0E-04	4
Arv S.		3.7	0.6	13.7	***E***	1.4	496.1		49.6	266.5		26.7	56.0	5.6	4.6E-09	8.5E-09		1.6E-05	1.9E-04	5.9E-04	4.3E-09	5.4E-04	4
Volv E.		4.9	0.7	13.7	***E***	1.4	505.9		50.6	291.6	***E***	29.2	60.9	6.1	3.4E-09	7.6E-09	5.1E-10	1.5E-05	1.6E-04	5.5E-04	6.6E-09	5.2E-04	3
Gou.		4.1	0.5	13.7	***E***	1.4	526.5		52.7	252.7		25.3	60.8	6.1	6.8E-09	7.9E-09	2.3E-10	1.5E-05	1.2E-04	5.6E-04	4.8E-09	6.1E-04	4
Chap.	**Down-stream catchement**	3.9	0.5																				
Pal.		4	0.5	10.9	***E***	1.1	525.1		52.5	330.0	***E***	33.0	44.0	4.4	6.9E-09	7.6E-09		1.4E-05	2.9E-05	5.5E-04	6.3E-09	7.0E-04	3
Garg.		3.9	0.5																				
Mean		*3.8*		*15.6*			*520.7*			*296.8*			*59.2*		*1.2E-08*	*7.9E-09*	*4.4E-10*	*1.5E-05*	*1.2E-04*	*5.6E-04*	*5.8E-09*	*4.8E-04*	
Std. Dev.		*0.5*		*3.2*			*19.6*			*50.2*			*7.0*		*1.4E-08*	*4.8E-10*	*1.2E-10*	*4.2E-07*	*7.2E-05*	*2.0E-05*	*1.9E-09*	*1.6E-04*	
field campaign 3 - February 2023																							
Maar	**Upstream catchement**	3.1	0.5	16.4	***E***	1.6	506.7		50.7	317.8	***E***	31.8	65.5	6.6	2.7E-09	9.7E-09	2.7E-09	1.6E-05	3.1E-04	6.4E-04	9.7E-10	2.3E-04	3
P10		2.4	0.4	24.6	***E***	2.5	524.3		52.4	251.6		25.2	70.1	7.0	2.9E-09	6.8E-09	2.6E-10	1.2E-05	2.8E-04	4.2E-04	3.1E-08	2.2E-04	4
M.Marc		2.7	0.4	16.4	***E***	1.6	516.5		51.6	263.8	***E***	26.4	63.2	6.3	2.6E-09	8.6E-09	5.1E-09	1.3E-05	2.9E-04	5.8E-04	3.7E-09	1.7E-04	3
Lat.		2.6	0.4																				
N27		2.7	0.5																				
Clai.	**Mid-catchement**	3.4	0.6	13.7	***E***	1.4	513.5		51.4	256.8		25.7	55.4	5.5	8.6E-09	8.9E-09	8.9E-08	1.6E-05	3.2E-04	6.3E-04	2.9E-09	2.3E-04	4
Aub.		2.7	0.4	10.9	***E***	1.1	511.0		51.1	274.6	***E***	27.5	74.7	7.5	5.0E-09	9.1E-09	1.9E-10	1.5E-05	3.3E-04	6.1E-04	3.6E-09	5.4E-04	3
Arv.		3.3	0.5	16.4	***E***	1.6	497.1		49.7	252.0		25.2	74.5	7.5	5.0E-09	9.1E-09	9.3E-08	1.5E-05	3.3E-04	6.1E-04	3.6E-09	4.2E-04	4
Arv S.		2.7	0.5	16.4	***E***	1.6	508.4		50.8	259.2		25.9	59.1	5.9	4.3E-09	6.8E-09	6.2E-08	1.2E-05	3.3E-04	4.2E-04	3.2E-09	5.1E-04	4
Volv E.		2.8	0.5	13.7	***E***	1.4	499.8		50.0	268.1		26.8	58.8	5.9	3.1E-09	8.7E-09	4.1E-10	1.5E-05	3.0E-04	6.1E-04	3.2E-09	4.1E-04	4
Gou.		2.7	0.4	13.7	***E***	1.4	498.8		49.9	238.8		23.9	64.5	6.5	6.2E-09	8.9E-09	3.4E-07	1.6E-05	3.1E-04	6.3E-04	2.7E-09	4.7E-04	4

(*continued on next page*)

Table 3 (*continued*)

Sample ID	Location	^3H	±	SF_6		±	CFC-12	±	CFC-11		±	CFC-113	±	He	Ne	H_2	Ar	O_2	N_2	CH_4	CO_2	Number of valid tracers
		(TU)		*(pptv)*										*(mol.L^{-1})*								
Chap.	**Down-stream**	2.9	0.4																			
Pal.	**catchement**	3.4	0.5	13.7	***E***	1.4	530.8		346.6	***E***	34.7	64.2	6.4	*7.6E-09*	*8.5E-09*	*2.2E-09*	*1.5E-05*	*2.6E-04*	*6.1E-04*	*3.7E-09*	*6.0E-04*	3
Garg.		2.6	0.5																			
Mars.		3.2	0.5	10.9	***E***	1.1	531.2		360.5	***E***	36.0	66.8	6.7	*5.2E-09*	*9.2E-09*	*2.2E-10*	*1.5E-05*	*2.3E-04*	*6.4E-04*	*2.8E-09*	*6.2E-04*	3
Mean		*2.9*		*15.2*			*512.6*		*280.9*			*65.2*		*4.8E-09*	*8.6E-09*	*5.4E-08*	*1.5E-05*	*3.0E-04*	*5.8E-04*	*5.6E-09*	*4.0E-04*	
Std. Dev.		*0.3*		*3.7*			*12.2*		*41.3*			*6.2*		*2.0E-09*	*9.4E-10*	*1.0E-07*	*1.4E-06*	*3.2E-05*	*8.0E-05*	*8.5E-09*	*1.6E-04*	
All campaigns																						
Mean		*3.3*		*15.4*			*516.4*		*288.5*			*62.3*		*8.17E-09*	*8.27E-09*	*3.53E-08*	*1.48E-05*	*2.14E-04*	*5.71E-04*	*5.69E-09*	*4.40E-04*	
Std. Dev.		*0.6*		*3.4*			*16.3*		*45.3*			*7.1*		*1.03E-08*	*8.10E-10*	*8.54E-08*	*1.01E-06*	*1.06E-04*	*5.95E-05*	*6.28E-09*	*1.60E-04*	

E: excess (for CFC-SF_6) = samples are considered in excess when their concentration is higher than the atmospheric maximum measured: 272.18 pptv for CFC-11, 546.18 pptv for CFC12 and 85.15 pptv for CFC-113 in the northern hemisphere (source NOAA).

this homogeneity, groundwater exhibits a slight increase in electrical conductivity across the catchment, from upstream to downstream, that can be attributed to water/rock interaction or, most probably, to inputs of surface water downstream the water basin. Rouquet (2012) opted for this hypothesis by showing both the impact of wastewater and agricultural activities on the nitrate and chloride signal in the upper part of the basin, and the influence of the road salting process on chloride levels in water bodies along the mid and downstream part of the catchment (Aub., Arv., Arv S., Volv E.). An enrichment in Cl^- and NO_3^- could be noticed for some points as P10, enriched in nitrate due to its location in an agricultural sector. More so, the mid and down parts of the catchment exhibit chloride inputs in relation with winter salt spreading of road during winter (Joux, 2002; Rouquet, 2012). Leaks within the local waste water network could also contribute to the abnormal concentrations in Cl^- observed at the outlets of the system: Garg., Pal., Chap.

Chemical composition of samples of higher water campaigns (Jun-22 and Oct-22) are slightly more widespread.

3.3.2. *Stable isotopic composition of groundwaters*

$\delta^{18}O$ and δ^2H values (Table. 2) range from −7.8 ‰ to −8.8 ‰ with an average of −8.5 ± 1.1 ‰ and from −50.3 ‰ to −58.0 ‰ with average about −56.0 ± 0.2 ‰, respectively. Almost all groundwaters are clustered close to the GMWL (GMWL: $\delta^2H = 8\delta^{18}O + 10$; Craig, 1961), and the Local Meteoric Water Line defined ($\delta^2H = 8.09\delta^{18}O + 13$), the latter being similar to the one proposed by Fouillac, 1991. It indicates that the recharge of groundwater originates from local precipitation. Groundwater is depleted compared to rainwaters collected in the central part of the basin (761 mNGF – Table 2), showing that main recharge occurs at higher altitude. Jun-22 and Oct-22 higher waters show a slight enrichment for some points. Despite this observation, stable isotopes of the water molecule indicate a homogeneous recharge at high altitude.

3.3.3. *Residence Time indicators: Tritium (^3H) and Chlorofluorocarbons (CFCs)*

Tritium (Table 3) ranges from 2.4 to 4.1 TU, with a mean of 3.3 ± 0.6 TU. The lowest values are recorded for Feb-2023 campaign, P10 is characterized by 2.4 TU. Oct-2022 present higher values, with a maximum of 4.1TU at Clai. and Gou. Despite these slight variations, tritium values appear to be homogeneous and not influenced by geographical distribution of water. Groundwater shows tritium contents below the atmospheric average for the Northern Hemisphere in 2021 (Vienna GNIP station), which is around 8.2 TU (IAEA/WMO (2024). Global Network of Isotopes in Precipitation. The GNIP Database. Accessible at: https://nucleus.iaea.org/wiser).

The equilibrium concentration of CFCs in groundwater depends on air pressure (i.e., altitude) and temperature in the saturated zone (pressure and temperature dependent – Henry's Law). It is then necessary to determine the elevation and the temperature of the recharge to estimate groundwater ages from CFC concentrations. The recharge temperature can be determined at 10.6 ± 2 °C by using noble gases Ne, Ar and N_2 (following Busenberg and Plummer, 1992; Plummer et al., 2012). This temperature is close to the annual air temperature recorded at Volvic weather station (9.4 ± 6.9 °C period: 1959–2023) and mean temperature of groundwater recorded through CTD probes during the period from June 2022 to October 2023 (9.2 ± 0.6 °C). Recharge temperature corresponds to the temperature in the recharge zone at the time of isolation of waters from the atmosphere during recharge. Therefore, it was chosen to use a recharge temperature of 9.2 °C, which corresponds to the average annual temperature of groundwaters in Volvic and remains coherent with annual atmospheric average and the recharge temperature given by noble gases. The selected recharge altitude corresponds to the average altitude of the upstream and mid-catchment parts of the catchment, considering that most of the recharge takes place in the upper half of the catchment (Joux, 2002). Microbial degradation of CFCs in a reducing environment (Cook et al., 1995; Shapiro et al., 1997; Sebol et al., 2007; Lapworth et al., 2018; Chambers

Table 4
February 2023 multi-tracer ^{3}H-CFC-113 MRTs (in years) based on Piston Flow Model (PFM).

Multi-tracer ^{3}H-CFC113 MRTs years based on *PFM model*				
	Sample ID	**Location**	**Mean age**	**Relative error (%)**
field campaign - February 2023	**Maar**	**Upstream**	**34**	0.05
	P10	**catchement**	**32**	0.17
	M.Marc		**35**	0.08
	Clai.	**Mid-catchement**	**35**	0.24
	Aub.		**35**	0.03
	Arv.		**33**	0.07
	Arv S.		**35**	0.01
	Volv E.		**33**	0.01
	Gou.		**35**	0.10
	Pal.	**Down-stream**	**35**	0.13
	Mars.	**catchement**	**34**	0.06
	Mean		*34.2*	
	Std. Dev.		*1.2*	

and Gooddy, 2019) can be excluded in the light of the dissolved oxygen concentrations measured as they are higher than 6.25×10^{-5} mol. L^{-1} (i.e., 2.0 mg. L^{-1}; Table 3).

Regarding chlorofluorocarbons, only CFC-11 exhibit slight excesses (except for P10 with a small CFC-12 excess in October 2022; Table 3). For SF_6, all samples display clearly excess values than the ones expected for an equilibrium with atmosphere, highlighting a probable different origin for this component (e.g., geogenic; Busenberg and Plummer, 2000; Koh et al., 2007; Gourcy et al., 2009). Low He concentrations (Table 3) suggests a relative young age for groundwaters, in that there is no evidence of water with a high He content that has infiltrated the system, based on work from Kulongoski and Hilton, 2012 exploring sources of helium in groundwater, For each sample we systematically obtained a minimum three valid tracers (Table 3; except for P10 with two valid tracers). We decided to base our analysis on the CFC-113-^{3}H combination as it is systematically valid for each analysis (Table 3). CFC-113 present concentrations ranging from 44.0 to 74.7 pptv (under the determined recharge temperature and elevation) for all samples from the two sampling campaigns, with limited variability in concentrations within a given sampling campaign: means about 59.2 ± 7.0 pptv and 66.8 ± 6.2 pptv for October 2022 and February 2023 campaign respectively, illustrating a high degree of homogeneity in the concentrations obtained, regardless of their location within the catchment area. Higher water (Oct-22) presents values slightly lower than low water (Feb-23).

4. Discussion: Hydrogeological conceptual model of the Volvic aquifer system

Results present two antagonist behaviours of Volvic aquifer. On one hand, hydrodynamic data and temperature records by probe (discharge and groundwater level; Fig. 4) highlights reactivity within the system in response to rainfall event and seasonality (high and low flow periods). On the other hand, hydrochemical analysis and stable isotopes of the water molecule support a unique origin of the recharge of groundwaters, mainly at high altitude, with only slight changes during the travel time of groundwater. Thus, recharge occurs at the height of the volcanic edifices at the top of the catchment area ("scoria cones"). The chemical composition of groundwaters defines the homogeneity of the system throughout the catchment with very limited variability between samples, independent of the period of the year and the location within the watershed. This is consistent with the observations of Joux (2002) and Rouquet (2012). Beyond this homogeneity, groundwater exhibits slight increase in electrical conductivity across the catchment, attributed to water/rock interaction or, most probably, to inputs of surface water downstream the catchment.

To better constrain both the reactive hydrodynamic and the chemical homogeneity of the system, further work focuses on determining the mean residence time of groundwater within the Volvic aquifer system to propose a conceptual model of the hydrogeological functioning of the catchment.

4.1. Residence time model (CFCs & Tritium) and mean residence times (MRTs)

Mean residence times (MRT) were calculated for groundwaters using ^{3}H and CFC-113 and tracer-tracer plots were used to identify the best lumped parameter model (LPM) to explain the results (Table 4 and Fig. 6). Fig. 6 a. and b. is a plot of CFC-113 against ^{3}H for Oct-2022 (orange symbols) and Feb-2023 (blue symbols) campaigns, respectively. Four mixing lines have been drawn in Fig. 6, each line representing a hypothetical mixing model: exponential model (EMM; red curve), piston flow model (PFM; blue curve) and two exponential piston model (EPM; green curves).

Concentrations of the samples collected during February 2023 are better explained by a Piston Flow Model (PFM). Mean Residence Times are calculated by using USGS TracerLPM calculation sheet (Jurgens et al., 2012, Fig. 6b - Table 4). As PFM implies an absence of mixing during the transit of groundwater, it is possible to determine the MRTs of the Volvic groundwater. This MRT corresponds to the duration of the transit time from the recharge by rainwater to the outlets downstream the water basin (case of captive or semi-captive aquifers with preferential recharge upstream of the catchment). Considering uncertainties, it is notable that observed ages are very homogeneous (32 to to 35 years) and seem to be independent of the location of the sampling point considered (Table 4). The average mean residence time is of 34,2 ± 1.2 years for the whole basin.

The most coherent model for Oct-2022 campaign is the Exponential Piston Model (EPM) with samples lying between different EPM ratios curves. Exponential Piston Model implies a contribution of an exponential recharge over the mid and downstream basin, due to infiltration of recent surface water, that mix with old water originated from the upper part of the basin. Most of the samples in Fig. 6a are located between EPM with ratio from 4 to 9, meaning that 10 % to 20 % of the model can be explained by Exponential Mixing Model and the remaining 80 %–90 % by a Piston Flow Model. This assumes that most groundwater sampled in Oct-2022 is the result of 10 to 20 % (even 30 % for 2 points) of recent water mixing with 80 to 90 % of old water. Some samples Aub., Clai. and Volv. appear to be more affected by the exponential contribution (up to 30 %).

4.2. Groundwater flowpaths, residence time and mixing: Hydrogeological conceptual model

The model proposed in Fig. 7 is an attempt to explain all the previous features, integrating geological, hydrogeological and climatic conditions together with the homogenous chemistry and the hydrodynamic variability. It considers:

- The upper part, characterized by highest recharge (due to the altitudinal gradient around 42 mm/ 100 m) that presents a low temperature. This high recharge infiltrates the cones and underlying structure (in blue Fig. 7) that cover an area of 15 km^2 with an estimated volume of material of 0.99 km^3. The effective porosity of these formations is of 40 to 45 % (Joux, 2002; Rouquet, 2012; Aumar, 2022). Recharge occurs preferentially in this part of the catchment at a low temperature due to altitude (Joux, 2002; Bertrand, 2009). Taking into account the high recharge, the volume and the porosity of these cones, recharge reach slowly the vadose zone where groundwater circulate through a Piston Flow Model with a mean residence time up to 35 years. This part of the system produces the "old component" of the aquifer.

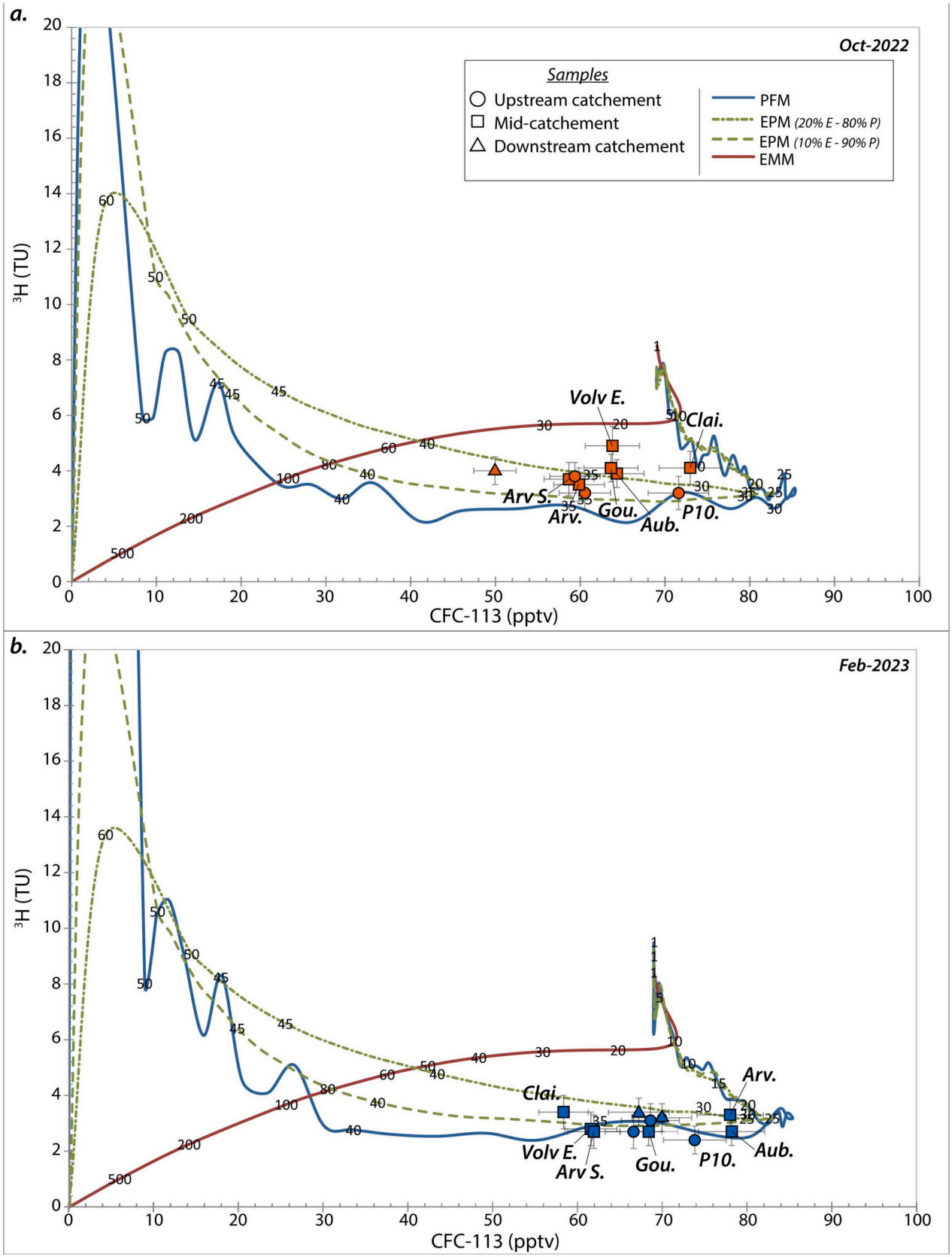

Fig. 6. : ^{3}H (TU) vs CFC-113 (pptv) in groundwater samples with a. field campaign of October 2022 and b. field campaign of February 2023. Theoretical curves are shown for piston flow model (PFM; blue), exponential mixing model (EMM; red), exponential piston flow model (EPM; green). The numbers on the lines are groundwater ages in years. EPM is represented with different curves corresponding to different ratio as follow: 4 (80 % piston – 20 % exponential) and 9 (90 % piston – 10 % exponential).

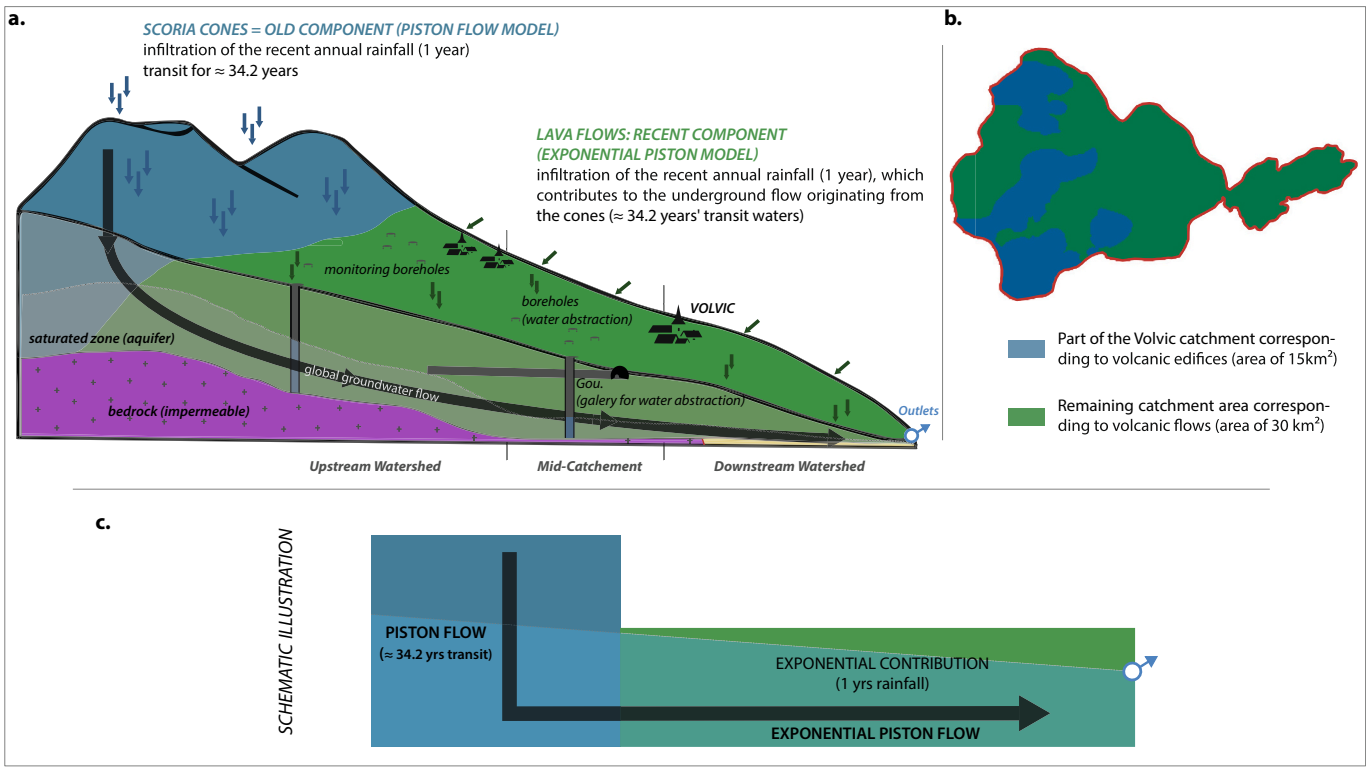

Fig. 7. :a.Conceptual hydrogeological model of the Volvic aquifer system b. Volvic catchment area and surface distribution between volcanic edifices (scoria cones) and the rest of the catchment area.

- The middle and lower parts (in green Fig. 7) cover an area of 30 km^2, elongated from west to east, for a volume of 1 km^3 and consist of lava flows separated from each other by their scoriaceous bases. The porosity and permeability of these materials are about 15 % and 10^{-3} to 10^{-5} m.s^{-1} respectively (Joux, 2002; Rouquet, 2012; Aumar, 2022). These hydrodynamic properties restrict the volumes of recharge that can potentially be stored and then recharge correspond to annual precipitation aging <1 year. Taking into account the low permeability of lava flows, rainwater preferentially infiltrates at the bedrock/lava flow contact (Rouquet, 2012). This part of the system produces the "recent component" of the aquifer which follows an exponential mixing model with contribution along the multi-layered volcanic aquifer.

Volvic catchment is therefore characterized by a Piston-Exponential Model (Fig. 7) into which the groundwater flowing through the Piston Flow Model of the upper part, is completed by groundwater from the mid and lower parts of the catchment, infiltrating according to an Exponential Mixing Model. This latter contribution is variable depending on the period (high/low waters) and the location of the sampling. For the campaign carried out during the study (Oct-2022 and Feb-2023), CFC-Tritium datation demonstrates that this part of recent component can vary from 10 to 30 %, with respectively 90 to 70 % of old component.

4.3. Limits of the methods and validation of the proposed hydrogeological model

Some hindsight is required on the MRTs given, as there may be biases in the measurements due to several factors; shifts in residence times may be induced by the solubility of gases, diffusion coefficients and soil water content (Cook and Herczeg, 2000; Heaton and Vogel, 1981), geology (Cook et al., 1995; Cook et al., 2006), and possible problems of contamination by external discharges and human activities such as gardening (Busenberg and Plummer, 2000; Spurlock et al., 2000). The thickness of the unsaturated zone (UZ) can also play a role, as the transport of gases may be affected depending on its thickness due to sorption into solid phase particles and potential microbial degradation, and therefore affect the interpretation of the residence time of CFCs. Indeed, influence of the UZ can be significant when interpreting gas tracers such as CFCs: processes like gas exchange, diffusion, and storage, can introduce delays or modify the concentrations of these tracers before they reach the water table (Cook et al., 1995; Cook and Solomon, 1995; Cook and Solomon, 1997; Gooddy et al., 2006). Such insights are critical for refining groundwater age models, particularly in complex geological settings, as neglecting these processes can result in inaccurate interpretations of groundwater residence times (Gooddy et al., 2006). However, the uncertainties introduced by the UZ can be minimized, improving the reliability of groundwater dating. In the present case, the use of multiple tracer (here CFC-113 and ^{3}H) helps cross-validate results as they exhibit different diffusion properties and they reduce reliance on a single tracer. In this way, Gooddy et al. (2006) suggest several solutions and approaches to address the influence of the unsaturated zone on, ensuring more accurate interpretations of groundwater age. In the case of Volvic, more detailed characterisation of the UZ through understanding its physical properties, such as thickness, gas diffusion rates, water content and soil composition can help predict tracer transport and potential delays. This can be achieved by field measurements or numerical modelling.

In addition, it is important to consider that estimating the temperature and altitude of the recharge zone also introduces a bias into the initial CFCs concentrations determined. Alongside, reductive conditions within the Volvic aquifer exclude potential microbial degradation of CFCs (Rowland and Molina, 1975; Cook and Solomon, 1995). In addition, the slight discrepancy between the estimated recharge temperatures using noble gases and the groundwater temperatures measured in situ using CTD-Diver probes shows that the chosen recharge temperature is consistent. Data uncertainty includes a 10 % bias on CFC

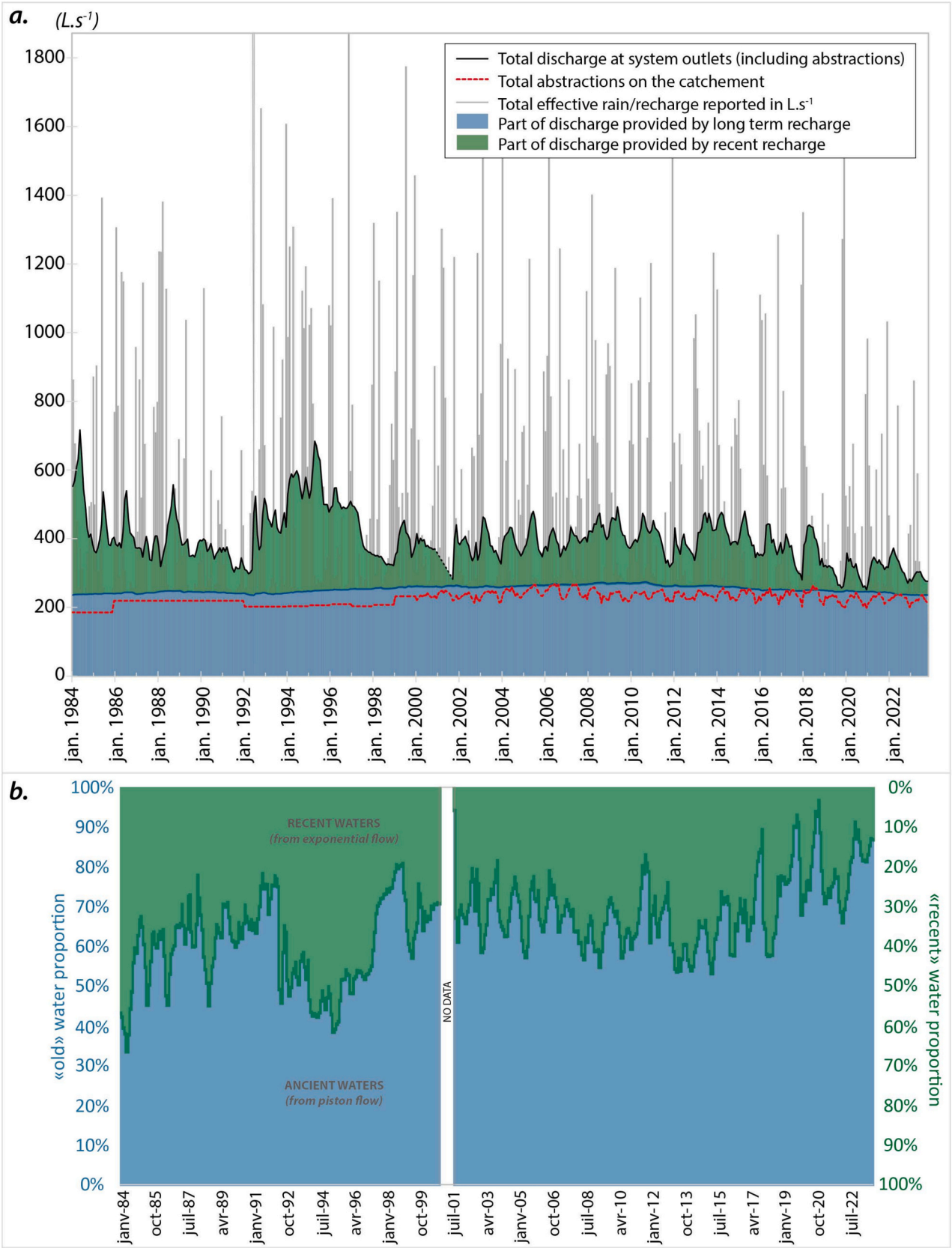

Fig. 8. : a. Discharge at Volvic system outlets with subdivision between sustained flow in blue and annual flow in green b. Changes in the proportion of recent (exponential) vs. old (piston) water over the last 30 years.

concentrations, to account for both variability in the analysis and variability in the recharge temperature. This bias is therefore already included in our interpretations and conclusions, which demonstrate consistency between the spatial distribution of ages and the observed homogeneity of the water mass given its chemical and isotopic composition.

As far as the temporal and hydrodynamic aspects are concerned, it can be seen that by assessing the percentages of contribution from recent and old waters, there is no 100 % contribution in February 2023, as it would be expected for a Piston Flow Model as described in the MRTs computation (Fig. 6b; Table 4). However, the piston model is approached to within 10 %, given that it is necessary to take into account the range of error induced by measurements, analysis and computations. Additionally, the 100 % piston model is an extremely rare occurrence in the nature, so it is very probable that there will always be a slight exponential contribution of 5 to 10 % on a model associated with piston functioning.

The model can then be validated by hydrodynamic data.

Taking into account the previous results, the contribution of old component (in blue, Fig. 8a) to the total discharge of the system (black curve) has been computed for the 1984–2023 period. The total discharge corresponds to natural discharge plus the extracted discharge for abstractions (red curve, Fig. 8a). The "old component" has been computed by considering the recharge 34.2 years ago. Thus, the flow from the old recharge in 1984 corresponds to the moving average over 34.2 years of recharge, i.e. since 1950 over the area of the scoria cones (blue zone, Fig. 8a), according to altitude gradient of the recharge (42 mm/100 m). The difference between the system's total discharge and old component corresponds to "recent component" (in green, Fig. 8a). Fig. 8a shows that total discharge during low-water periods is mainly derived from old component while the contribution of recent component increases during high waters and can even be predominant in comparison to old component in some periods (e.g. in 1992–1994). Estimation of the proportions of old component through these computations indicates that old component accounts for 83 to 88 % of the total discharge for Oct-2022 and Feb-2023 respectively, confirming the results obtained by datation (considering here uncertainty induced by discharge measurements and recharge computations).

Fig. 8a and b highlights moreover the decreasing trend of the total discharge of Volvic hydrosystem in relation with the reduction of the recent component, directly linked to the recent increase in mean atmospheric temperatures due to global change (IPCC: Climate Change, 2021). This recharge decrease should however be considered over time as it might affect the old component in 30 years.

5. Conclusion & perspectives on water resource management

From a technical perspective, this study demonstrates the importance of using a combination of geological, hydrogeological and geochemical approaches, including the use of environmental tracers. For the latter, the decrease in atmospheric CFC and tritium levels, the variability of tritium levels in recent years, and the sensitivity of certain CFCs and SF_6 to contamination (excess values) confirmed the need to use several tracers, namely the CFC-113-Tritium combination in this study. This study also demonstrated the applicability of environmental tracers in the context of exploited volcanic aquifers.

Findings presented in this work demonstrated the homogeneity of the Volvic aquifer system in all seasons, through a homogeneous chemical and isotopic composition that remains stable over time. System reactivity, as evidenced by piezometric variations and more importantly discharge variations at the system's outlets, which seemed to contradict the system's previously proposed homogeneity, can be explained by the results of CFC-113-^{3}H dating. This datation revealed that the aquifer system is composed of "old" water, with a mean residence time (MRT) approaching 34.2 years (s.d: 1.2), acquired during the groundwater's transit through the scoriaceous volcanic edifices (= the piston part of the model). This "old" component is supplemented by a contribution from recent water (surface water from precipitation; exponential part of the model), supplying the system through the lava layers that constitute the rest of the aquifer system, beyond volcanic edifices. This "recent" input is variable according to the location within the catchment area, with some locations being more sensitive to the inflow of recent surface water (e.g. sampling points Aub., Clai. and Volv, supported by Rouquet, 2012). Recent contribution also fluctuates according to the season/time of year, with a more significant contribution during high-water periods. Finally, it has been demonstrated that this contribution of recent water may have been predominant over the past (during the last thirty years) and it is important to point out that over the last 10 years, this recent contribution seems to decrease in conjunction with increasing atmospheric temperatures. It is therefore important to consider this decrease of the recent input over time, in the light of the ongoing climate change and the current pressures on water resources at the Volvic catchment.

With regard to water resource management, these observations provide an opportunity to assess, and possibly re-evaluate, the share of current water abstractions within the overall aquifer system. At present, it would appear that these withdrawals are assured/compensated for by the contribution of old recharge. But suppose the recent recharge decreases drastically (rise in temperatures-climate change), this could threaten the system's outlets, which would no longer be supplied (the old recharge having itself been impacted over the long term). At that point, it could be expected that there would be not enough water to ensure not only the discharge at the system's outlets, but also all the abstractions at their current rates. For the purposes of preventing and anticipating these threats, integrating this conceptual model for hydrological modelling to predict future changes in water resources could be extremely valuable.

CRediT authorship contribution statement

Pierre Nevers: Writing – original draft, Visualization, Validation, Supervision, Resources, Investigation, Funding acquisition, Formal analysis, Conceptualization. **Hélène Celle:** Writing – original draft, Validation, Supervision, Resources, Project administration, Funding acquisition, Formal analysis, Conceptualization. **Cyril Aumar:** Writing – review & editing, Investigation. **Virginie Vergnaud:** Writing – review & editing, Resources, Investigation. **Barbara Yvard:** Writing – review & editing, Resources, Investigation. **Gilles Mailhot:** Writing – review & editing, Project administration.

Funding sources

This research was financially supported by Agence de l'Eau Loire Bretagne, Préfecture du Puys de Dôme (Direction des Départements et des Territoires 63), Communauté d'agglomération Riom Limagne et Volcans and Syndicat Mixte des Utilisateurs d'Eau de la Région de Riom.

Declaration of competing interest

The authors declare that they have no known competing financial interests or personal relationships that could have appeared to influence the work reported in this paper.

Acknowledgements

Caroline Amiot, Nadia Crini and Christophe Loup are acknowledged for analytical support. Victor Klaba is acknowledged for support on the field. The authors thank the PEA^{2}t platform (Chrono-Environment, Université de Bourgogne Franche-Comté, UMR CNRS 6249, France), which manages and maintains the analytical equipment used in this study for major element analyses.

Data availability

Data will be made available on request.

References

Arnell, N., Detlef, P. van V., Morna, I.: the implications of climate policy for the impacts of climate change on global water resources. Glob. Environ. Chang., 21, 592–603, https://doi.org/10.1016/j.gloenvcha.2011.01.015, 2011.

Ascott, M., Macdonald, D.M.J., Sandwidi, W.J.P., Black, E., Verhoef, A., Zongo, G., Tirogo, J., Cook, P., 2022. Time of emergence of impacts of climate change on groundwater levels in sub-Saharan Africa. J. Hydrol. 612, 128107. https://doi.org/10.1016/j.jhydrol.2022.128107.

Aubignat, A., 1973. Le gisement hydrominéral de Volvic. Revue Scientifique et Naturelle d'Auvergne, 29–32.

Aumar, C., 2022. Modélisation de la topographie anté-volcanique de la Chaîne des Puys : Implications hydrogéologiques pour les bassins versants de la Veyre et de Côme. PhD Thesis,. Université Clermont Auvergne.

Aumar, C., Labazuy, P., Merle, O., Buvat, S., & Merciecca, C. Prevolcanic Topography and Hydrogeological Watershed of the Chaîne Des Puys [Data Set]. OPGC, LMV. doi:10.25519/R1PR-G644, 2024.

Ayraud, V., Aquilina, L., Labasque, T., Pauwels, H., Molenat, J., Pierson-Wickmann, A.-C., Durand, V., Bour, O., Tarits, C., Le Corre, P., Fourre, E., Merot, P., Davy, P., 2008. Compartmentalization of physical and chemical properties in hard-rock aquifers deduced from chemical and groundwater age analyses. Appl. Geochem. 23, 2686–2707. https://doi.org/10.1016/j.apgeochem.2008.06.001.

Barbaud, J.Y. : Etude chimique et isotopique des aquifères de la Chaîne des Puys, temps de transit et vulnérabilité des systèmes de Volvic et d'Argnat. Thèse de 3ième cycle, Faculté des Sciences d'Avignon, Avignon, 209 pp, 1983.

Baud, B., 2024. Characterisation of Andesitic Volcanic Aquifers through a Multidisciplinary Approach, Conceptual Model. PhD Thesis,. Université de Montpellier.

Baulon, L., 2023. Déterminisme climatique et hydrogéologique de l'évolution à long terme des niveaux piézométriques. Sciences de la Terre, PhD Thesis, Normandie Université. NNT. NORMR015. tel-04123371, 292p.

Belin, J.M., Livet, M., Heraud, H., Clermont-Ferrand, Autoroute Périgueux, 1988. Dossier d'étude préliminaire de la Chaîne des Puys. Ministère de l'équipement et du Logement, CETE Lyon, laboratoire régional de Clermont-Ferrand, 167p.

Belkessa, R., 1977. Hydrogéologie de la Chaîne des Puys. D.E.S. Univ. Cl-Fd, Université de Clermont-Ferrand.

Bertrand, G., 2009. De la pluie à l'eau souterraine : Apport du traçage Naturel (ions majeurs, isotopes) à l'étude du fonctionnement des aquifères volcaniques (Bassin d'Argnat, Auvergne France). PhD Thesis,. Université Blaise Pascal, Clermont-Ferrand II.

Bertrand, G., Celle-Jeanton, H., Huneau, F., Loock, S., Renac, C., 2010. Identification of different groundwater flowpaths within volcanic aquifers using natural tracers for the evaluation of the influence of lava flows morphology (Argnat basin, Chaîne des Puys, France). J. Hydrol. 391, 223–234.

Boivin, P., Thouret, J.C., Briot, D., Deniel, C., Gourgaud, A., Labazuy, P., De Larouzière, F.D., Livet, M., Médard, E., Merciecca. C., Mergoil, J., Miallier, D., Morel, J.M., Thouret, J.C., Vernet, G.: Carte volcanologique de la Chaîne des Puys, 6th ed, 2017.

Bouchet, C. : Hydrogéologie du milieu volcanique, le bassin de la Veyre, analyse et modélisation du bassin versant du lac d'Aydat, étude d'un aquifère fissuré basaltique. Thèse de doctorat, Université d'Avignon et des Pays de Vaucluse, Avignon, 319 pp, 1987.

Bu, X., Warner, M.J., 1995. Solubility of chlorofluorocarbon 113 in water and seawater. Deep Sea Res. Part I. Oceanograph. Res. Papers 42 (7), 1151–1161. https://doi.org/10.1016/0967-0637(95)00052-8. ISSN 0967-0637.

Bullister, J.L., Wisegarver, D.P., Menzia, F.A., 2002. The solubility of sulfur hexafluoride in water and seawater. Deep Sea Res. Part I. Oceanograph. Res. Papers 49 (1), 175–187. https://doi.org/10.1016/S0967-0637(01)00051-6. ISSN 0967-0637.

Busenberg, E., Plummer, L.N., 1992. Use of chlorofluorocarbons (CCl3F and CCl2F2) as hydrologic tracers and age-dating tools: the alluvium and terrace system of Central Oklahoma. Water Resour. Res. 28 (9), 2257–2283. https://doi.org/10.1029/92WR01263.

Busenberg, E., Plummer, L.N., 2000. Dating young ground water with sulfur hexafluoride - natural and anthropogenic sources of sulfur hexafluoride. Water Resour. Res. 36, 3011–3030. https://doi.org/10.1029/2000WR900151.

Camus, G. : La Chaîne des Puys (Massif Ce,tral Français) étude structurale et volcanologique. Thèse d'Etat, UEF Sciences exactes et Naturelles, université de Clermont-Ferrand, 322 pp, 1975.

Canellas, C., Gibelin, A.L., Lassegues, P., Kerdoncuff, M., Dandin, P., Simon, P. : Les normales climatiques spatialisées Aurelhy 1981–2010 : températures et précipitations. La Météorologie, 8, 47, https://doi.org/10.4267/2042/53750, 2014.

Celle-Jeanton, H., Bertrand, G., Loock, S., Huneau, F., 2008. Conditions d'alimentation et vulnérabilité des sources de bout de coulées volcaniques de la Chaîne des Puys: exemple du bassin d'Argnat. Géologues 15, 9–13.

CETE/LRPC: Bilan de la resource hydrogéologique des bassins de la Chaîne des Puys, Lyon, 2009.

Chambers, L.A., Gooddy, D.C., Binley, A., M., 2019. Use and application of CFC-11, CFC-12, CFC-113 and SF6 as environmental tracers of groundwater residence time: a review. Geosci. Front. 10 (5), 1643–1652. ISSN 1674-9871,. https://doi.org/10.1016/j.gsf.2018.02.017.

Chatton, E., Aquilina, L., Pételet-Giraud, E., Cary, L., Bertrand, G., Labasque, T., Hirata, R., et al., 2016. Glacial recharge, salinisation and anthropogenic contamination in the coastal aquifers of Recife (Brazil). Sci. Total Environ. 569–570 (November), 1114–1125. https://doi.org/10.1016/j.scitotenv.2016.06.180.

Colombier, M., Gurioli, L., Druitt, T.H., et al., 2017. Textural evolution of magma during the 9.4-ka trachytic explosive eruption at Kilian volcano, Chaîne des Puys, France. Bull. Volcanol. 79, 17. https://doi.org/10.1007/s00445-017-1099-7.

Cook, P., Herczeg, A., 2000. Environmental Tracers in Subsurface Hydrology. https://doi.org/10.1007/978-1-4615-4557-6.

Cook, P.G., Solomon, D.K., 1995. Transport of atmospheric trace gases to the water table: implications for groundwater dating with chlorofluorocarbons and krypton 85, water Resour. Res 31 (2), 263–270. https://doi.org/10.1029/94WR02232.

Cook, P., Solomon, D., Plummer, L., Busenberg, E., Schiff, S., 1995b. Chlorofluorocarbons as tracers of groundwater transport processes in a shallow, silty sand aquifer. Water Resour. Res. 31, 425–434. https://doi.org/10.1029/94WR02528.

Cook, P.G., Plummer, L.N., Busenberg, E., Solomon, D.K., Han, L.F., Chapter 4: Effects and processes that can modify apparent CFC age. Use of chlorofluorocarbons in hydrology: A guidebook. International Atomic Agency, STI/PUB/1238, Vienna, ISBN 92-0-1000805-8, 2006.

Cook, P.G., Solomon, D.K., 1997. Recent advances in dating young groundwater: chlorofluorocarbons, 3H3He and 85Kr. J. Hydrol. 191 (1–4), 245–265. ISSN 0022-1694,. https://doi.org/10.1016/S0022-1694(96)03051-X.

Cosgrove, W.J., Loucks, D.P., 2015. Water management: current and future challenges and research directions. Water Resour. Res. 51, 4823–4839. https://doi.org/10.1002/2014WR016869, 2015.

Cotterman, K.A.; Kendall, A.D.; Basso, B.; Hyndman, D.W. Groundwater depletion and climate change: future prospects of crop production in the central High Plains aquifer. Clim. Chang., 146, 187–20, 2018.

Craig, H., 1961. Isotopic variations in meteoric waters. Science 133, 1702–1703.

Custodio, E., 1985. Low Permeability Volcanics in the Canary Islands (Spain).

Darling, W.G., Gooddy, Daren, Macdonald, Alan, Morris, B., L., 2012. The practicalities of using CFCs and SF6 for groundwater dating and tracing. Appl. Geochem. 27, 1688–1697. https://doi.org/10.1016/j.apgeochem.2012.02.005.

Dayon, G., Boe, J., Martin, E., Gailhard, J., 2018. Impacts of climate change on the hydrological cycle over France and associated uncertainties. Comptes Rendus Géoscience 350, 141–153. https://doi.org/10.1016/j.crte.2018.03.001.

Fouillac C., Fouillac, A.M., Chery, L.: Isotopic studies of deep and surface waters in the French Massif central. Proceedings of isotope techniques in water resources development. Vienne, 11–15 mars, p. 646–648, 1991.

Fournier, C., 1983. Méthodes géoélectriques appliquées à l'hydrogéologie en région volcanique (Chaîne des Puys, Massif Central Français). Développement de la méthode des potentiels spontanés en hydrogéologie. Thèse de 3ième cycle,. Université des Sciences et Techniques du Languedoc, Montpellier.

Gaubi, E.B., 1990. Etude hydrogéologique de l'extrémité aval du bassin d'Argnat (Chaîne des Puys, Massif Central Français). Projet de l'autoroute Périgueux-Clermont-Ferrand. Mémoire de DEA national d'hydrogéologie, Sciences de l'eau et aménagement. Besançon.

Gil-Márquez, J., M, Sültenfuß, J., Andreo, B., Mudarra, M., 2020. Groundwater dating tools (3H, 3He, 4He, CFC-12, SF6) coupled with hydrochemistry to evaluate the hydrogeological functioning of complex evaporite-karst settings. J. Hydrol. 580, 124263. ISSN 0022-1694,. https://doi.org/10.1016/j.jhydrol.2019.124263.

Githui, F., Mutua, F., Bauwens, W., 2009. Estimating the impacts of land-cover change on runoff using the soil and water assessment tool (SWAT): case study of Nzoia catchment, Kenya / estimation des impacts du changement d'occupation du sol Sur l'écoulement à l'aide de SWAT: étude du cas du bassin de Nzoia. Kenya. Hydrological Sciences Journal 54 (5), 899–908. https://doi.org/10.1623/hysj.54.5.899.

Gooddy, D.C., Darling, W.G., Abesser, C., Lapworth, D.J., 2006. Using chlorofluorocarbons (CFCs) and sulphur hexafluoride (SF6) to characterise groundwater movement and residence time in a lowland Chalk catchment. J. Hydrol. 330 (1–2), 44–52. https://doi.org/10.1016/j.jhydrol.2006.04.011. ISSN 0022-1694.

Gourcy, L., Baran, N., Vittecoq, B., 2009. Improving the knowledge of pesticide and nitrate transfer processes using age-dating tools (CFC, SF6, 3H) in a volcanic island (Martinique, French West Indies). J. Contam. Hydrol. 108 (3–4), 107–117. https://doi.org/10.1016/j.jconhyd.2009.06.004. ISSN 0169-7722.

Han, L., Hacker, P., Gröning, M., 2007. Residence times and age distributions of spring waters at the Semmering catchment area, eastern Austria, as inferred from tritium, CFCs and stable isotopes. Isot. Environ. Health Stud. 43, 31–50. https://doi.org/10.1080/10256010601154015.

Harris, A., Latutrie, B., Wyk, Van, de Vries, B., Saubin, E., Foucher, M., Gurioli, L., Zanella, E., Médard, E., Nauret, F., 2023. Emplacement of monogenetic lava flows on eroded terrain, part II: the case of the Artière valley (grave noire, France). J. Volcanol. Geotherm. Res. 438.

Heaton, T., Vogel, J., 1981. Excess air in groundwater. J. Hydrol. 50, 201–216. https://doi.org/10.1016/0022-1694(81)90070-6.

IAEA/WMO 2024 Global Network of Isotopes in Precipitation. The GNIP Database. Accessible at: https://nucleus.iaea.org/wiser.

IPCC: Climate Change 2021: The Physical Science Basis. Contribution of Working Group I to the Sixth Assessment Report of the Intergovernmental Panel on Climate Change [Masson-Delmotte, V., P. Zhai, A. Pirani, S.L. Connors, C. Péan, S. Berger, N. Caud, Y. Chen, L. Goldfarb, M.I. Gomis, *M. Huang*, K. Leitzell, E. Lonnoy, J.B.R. Matthews, T. K. Maycock, T. Waterfield, O. Yelekçi, R. Yu, and B. Zhou (eds.)]. Cambridge University Press, Cambridge, United Kingdom and New York, NY, USA, In press, https://doi.org/10.1017/9781009157896, 2021.

Janot, S. Genèse, et al., 2005. une approche par l'étude des inclusions magmatiques. Géologie appliquée. PhD Thesis, Université Blaise Pascal - Clermont-Ferrand II. NNT: 2005CLF21619. tel-00684061. In: évolution des magmas primitifs de la chaine des Puys (Massif Central).

Jasechko, S., Seybold, H., Perrone, D., Fan, Y., Shamsudduha, M., Taylor, R., Fallatah, O., Kirchner, J., 2024. Rapid groundwater decline and some cases of recovery in aquifers globally. Nature 625, 715–721. https://doi.org/10.1038/s41586-023-06879-8.

Josnin, J.Y., Livet, M., Besson, J.C., 2007. Characterizing unsaturated flow from packed scoriated lapilli: application to Strombolian cone hydrodynamic behaviour. J. Hydrol. 335, 225–239.

Joux, M., 2002. Structure et fonctionnement hydrogéologique du système aquifère volcanique des eaux minérales de Volvic (Chaîne des Puys, Massif Central Français). PhD Thesis,. Université d'Avignon et des Pays de Vaucluse.

Jurgens, B., Bohlke, J., Eberts, S., 2012. TracerLPM (Version 1): An Excel® workbook for interpreting groundwater age distributions from environmental tracer data. U.S. Geol. Surv. Tech. Methods Rep. 4-F3, 60. https://doi.org/10.3133/tm4F3.

Koh, D., C., Plummer, N., L., Busenberg, E., Kim, Y.: Evidence for terrigenic SF6 in groundwater from basaltic aquifers,Jeju Island, Korea: Implications for groundwater dating, J. Hydrol., Volume 339, Issues 1 2, Pages 93–104, ISSN 0022-1694, doi: https://doi.org/10.1016/j.jhydrol.2007.03.011, 2007.

Kulongoski, J.T., Hilton, D.R., 2012. Applications of groundwater helium. In: Baskaran, M. (Ed.), Handbook of Environmental Isotope Geochemistry. Advances in Isotope Geochemistry. Springer, Berlin, Heidelberg. https://doi.org/10.1007/978-3-642-10637-8_15.

Labasque, T., Ayraud, V., Aquilina, L., Corre, L., 2006. Dosage des composés chlorofluorocarbonatés et du tétrachlorure de carbone dans les eaux souterraines. Application à la datation des eaux. Cahiers techniques de Géosciences Rennes. No. 4.

Labbe, J., Celle, H., Devidal, J.L., Albaric, J., Mailhot, G., 2023. Combined impacts of climate change and water withdrawals on the water balance at the watershed scale - the case of the Allier alluvial Hydrosystem (France). Sustainability 15, 3275. https://doi.org/10.3390/su15043275.

Labrousse, C., Ludwig, W., Pinel, S., Sadaoui, M., Toreti, A., Lacquement, G., 2022. Declining water resources in response to global warming and changes in atmospheric circulation patterns over southern Mediterranean France. Hydrol. Earth Syst. Sci. 26, 6055–6071. https://doi.org/10.5194/hess-26-6055-2022.

Lachassagne, P., Aunay, B., Frissant, N., Guilbert, M., Malard, A., 2014. .High-resolution conceptual hydrogeological model of complex basaltic volcanic islands: a Mayotte, Comoros, case study. Terra Nova 26, 307–321.. https://doi.org/10.1111/ter.12102.

Lanini, S., Caballero, Y., Seguin, J.-J., Maréchal, J.-C., 2015. ESPERE - a multiple-method Microsoft excel application for estimating aquifer recharge. Groundwater 54, 155–156. https://doi.org/10.1111/gwat.12390.

Lapworth, D.J., Das, P., Shaw, A., Mukherjee, A., Civil, W., Petersen, J.O., Gooddy, D.C., Wakefield, O., Finlayson, A., Krishan, G., Sengupta, P., MacDonald, A., M., 2018. Deep urban groundwater vulnerability in India revealed through the use of emerging organic contaminants and residence time tracers. Environ. Pollut. 240, 938–949. ISSN 0269-7491,. https://doi.org/10.1016/j.envpol.2018.04.053.

Le Bas, C. : "Carte de la Réserve Utile en eau issue de la Base de Données Géographique des Sols de France", doi:10.15454/JPB9RB, Recherche Data Gouv, V2, 2018.

Livet, M., Blavoux, B., d'Arcy, D., Mishellany, A., 2000. Capture and sub-lava storage of groundwater at the volcanic site of Beaunit (Puy-de-Dôme) / Capture et emmagasinement sous coulée au site volcanique de Beaunit (Puy-de-Dôme), Comptes Rendus de l'Académie des Sciences - Series IIA - Earth and Planetary. Science 330 (1), 47–52. ISSN 1251-8050,. https://doi.org/10.1016/S1251-8050(00)00123-3.

Loock, S., Celle-Jeanton, H., Bertrand, G., Van Wyk de Vries, B. : Les aquifères des coulées basaltiques. Réunion des Sciences de la Terre, Nancy, France, 21–24 avril 2008, presentation 29-d, 2008.

Lustrino, M., Wilson, M., 2007. The Circum-Mediterranean Anorogenic Cenozoic Igneous Province. Earth-science Reviews - EARTH-SCI REV. 81, 1–65. https://doi.org/10.1016/j.earscirev.2006.09.002.

Ma, B., Jin, M., Liang, X., Li, J., 2019. Application of environmental tracers for investigation of groundwater mean residence time and aquifer recharge in fault-influenced hydraulic drop alluvium aquifers. Hydrol. Earth Syst. Sci. 23, 427–446. https://doi.org/10.5194/hess-23-427-2019.

Magi, F., Doveri, M., Menichini, M., Minissale, A., Vaselli, O., 2019. Groundwater response to local climate variability: hydrogeological and isotopic evidences from the Mt. Amiata volcanic aquifer (Tuscany, Central Italy). Rendiconti Lincei. Scienze Fisiche e Naturali 30. https://doi.org/10.1007/s12210-019-00779-8.

Merle, O., Aumar, C., Labazuy, P., Merciecca, C., Buvat, S., 2023. Structuration tertiaire et quaternaire du Plateau des Dômes (Chaîne des Puys, Massif central, France). Géol. Fr. n°1,, 1–22.

Merle, O., Michon, L., 2001. The formation of the West European Rift; a new model as exemplified by the Massif Central area. Bulletin de la Société Géologique de France. 172 (2), 213–221. https://doi.org/10.2113/172.2.213.

Michel, R., 1957. Hydrogéologie des formations volcaniques de l'Auvergne. Bulletin de la Société Géologique de France 7, 977–994.

Murray, S.J., Foster, P.N., Prentice, I.C.: Future global water resources with respect to climate change and water withdrawals as estimated by a dynamic global vegetation model. Journal of Hydrology, Volumes 448–449, Pages 14–29, ISSN 0022–1694, https://doi.org/10.1016/j.jhydrol.2012.02.044, 2012.

Nearing, M., Jetten, V.G., Baffaut, C., Cerdan, O., Couturier, A., Hernandez, M., Le Bissonnais, Y., Nichols, M., Nunes, J.P., Renschler, C., Souchère, V., Oost, K.: Modeling Response of Soil Erosion and Runoff to Changes in Precipitation and Cover. Catena. 131–154. https://doi.org/10.1016/j.catena.2005.03.007, 2005.

Okofo, L., B., Adonadaga, M., G., Martienssen, M., 2022. Groundwater age dating using multi-environmental tracers (SF6, CFC-11, CFC-12, δ18O, and δD) to investigate groundwater residence times and recharge processes in northeastern Ghana. J. Hydrol. 610, 127821. ISSN 0022-1694,. https://doi.org/10.1016/j.jhydrol.2022.127821.

Oster, H., Sonntag, C., Münnich, K.O., 1996. Groundwater age dating with chlorofluorocarbons. Water Resour. Res. 32 (10), 2989–3001. https://doi.org/10.1029/96WR01775.

Oudin, L., Hervieu, F., Michel, C., Perrin, C., Andréassian, V., Anctil, F., Loumagne, C., 2005. Which potential evapotranspiration input for a rainfall-runoff model? Part 2 - Towards a simple and efficient PE model for rainfall-runoff modelling. J. Hydrol. 303 (1-4), 290–306.

Parajuli, P.B., 2010. Assessing sensitivity of hydrologic responses to climate change from forested watershed in Mississippi. Hydrol. Process. 24, 3785–3797. https://doi.org/10.1002/hyp.7793.

Penna, D., Stenni, B., Sanda, M., Wrede, S., Bogaard, T.A., Gobbi, A., Borga, M., Fischer, B.M.C., Bonazza, M., Charova, Z., 2010. On the reproducibility and repeatabilityof laser absorption spectroscopy measurements for delta H-2 and delta O-18isotopic analysis. Hydrol. Earth Syst. Sci. 14, 1551–1566. https://doi.org/10.5194/hess-14-1551-2010.

Pérotin, L, Montety, V de, Ladouche, B, Bailly-Comte, V, Labasque, T, Vergnaud, V, Muller, R, Champollion, C, Tweed, S, and Seidel, J-L.: "Transfer of dissolved gases through a thick karstic vadose zone – implications for recharge characterisation and groundwater age dating in karstic aquifers." J. Hydrol. 601 (October): 126576. doi: https://doi.org/10.1016/J.JHYDROL.2021.126576, 2021.

Plummer, L.N., Busenberg, E., Bohlke, J.K., Nelms, D.L., Michel, R.L., Schlosser, P., 2001. Groundwater residence times in Shenandoah National Park, blue Ridge Mountains, Virginia, USA: a multi-tracer approach. Chem. Geol. 179, 93–111. https://doi.org/10.1016/S0009-2541(01)00317-5.

Plummer, L.N., Busenberg, E., Cook, P.G., 2006. Chapter 3 Principles of Chlorofluorocarbon Dating. IAEA, International Atomic Energy Agency (IAEA).

Plummer, L.N., Eggleston, J.R., Andreasen, D.C., Raffensperger, J.P., Hunt, A.G., Casile, G.C., 2012. Old groundwater in parts of the upper Patapsco aquifer, Atlantic coastal plain, Maryland, USA: evidence from radiocarbon, chlorine-36 and helium-4. Hydrogeol. J. 20, 1269–1294. https://doi.org/10.1007/s10040-012-0871-1.

Poncela, R., Santamarta, J.C., García-Gil, A., Cruz-Pérez, N., Skupien, E., García-Barba, J., 2022. Hydrogeological characterization of heterogeneous volcanic aquifers in the Canary Islands using recession analysis of deep water gallery discharge. J. Hydrol. 610, 127975.

Prudhomme, C., et al.: Hydrological droughts in the 21st century, hotspots and uncertainties from a global multimodel ensemble experiment. Proceedings of the National Academy of Sciences of the United States of America, 111 (9), 3262–3267. National Academy of Sciences, https://doi.org/10.1073/pnas.1222473110, 2014.

Ranchoux, C., Chabaux, F., Viville, D., Labasque, T., Lucas, Y., Van der Woerd, J., Ackerer, J., Aquilina, L., 2021. Characterization of groundwater circulations in a headwater catchment from an analysis of chemical concentrations, Sr-Nd-U isotope ratios, and CFC, SF6 gas tracers (Strengbach CZO, France), applied geochemistry, volume 131, 105030. ISSN 0883-2927. https://doi.org/10.1016/j.apgeochem.2021.105030.

Rockström, J., Steffen, Noone, K., Persson, Å., Chapin III, F.S., Lambin, E.F., Lenton, T. M., Scheffer, M., Folke, C., Schellnhuber, H.J., Nykvist, B., de Wit, C.A., Hughes, T., Van der Leeuw, S., Rodhe, H., Sörlin, S., Snyder, P.K., Costanza, R., Svedin, U., Falkenmark, M., Karlberg, L., Corell, R.W., Fabry, V.J., Hansen, J., Walker, B., Liverman, D., Richardson, K., Crutzen, P., Foley, J.: A safe operating space for humanity. Nature, v.461, 472–475, 46, 2009.

Rouquet, S., 2012. Etude du fonctionnement hydrogéologique et modélisation de l'hydrosystème de Volvic : Prise en compte du rôle joué par la forêt. PhD Thesis,. Ecole Nationale Supérieure des Mines de Paris.

Rouquet, S., Boivin, P., Lachassagne, P., Ledoux, E., 2012. A 3-D genetic approach to high-resolution geological modelling of the volcanic infill of a paleovalley system. Application to the Volvic catchment (Chaîne des Puys, France). Bulletin de la Société Géologique de France 183, 395–407. https://doi.org/10.2113/gssgfbull.183.5.395.

Rowland, F.S., Molina, M.J., 1975. Chlorofluoromethanes in the environment. Rev. Geophys. 13 (1), 1–35. https://doi.org/10.1029/RG013i001p00001.

Sauquet, E., Beaufort, A., Sarremejane, R., Thirel, G., 2021. Predicting flow intermittence in France under climate change. Hydrol. Sci. J. 66 (14), 2046–2059. https://doi.org/10.1080/02626667.2021.1963444.

SDES, IGN, European Environment Agency, 2019. Occupation du sol - Corine land cover. SDES. https://doi.org/10.12770/ac797a9e-60b5-4e22-bd4c-df2f7a6fe217, 2018.

Sebol, L.A., Robertson, W.D., Busenberg, E., Plummer, L.N., Ryan, M.C., Schiff, S.L., 2007. Evidence of CFC Degradation in Groundwater under Pyrite-Oxidizing Conditions, Journal of Hydrology, Volume 347, Issues 1–2, Pages 1–12, ISSN 0022–1694. https://doi.org/10.1016/j.jhydrol.2007.08.009.

Shapiro, S.D., Schlosser, P., Smethie, W.M., Stute, M., 1997. The use of 3H and tritiogenic 3He to determine CFC degradation and vertical mixing rates in Framvaren Fjord. Norway. Marine Chemistry 59 (1–2), 141–157. https://doi.org/10.1016/S0304-4203(97)00007-8.

Shinhu, R.J., Amasi, A.I., Wynants, M., Nobert, J., Mtei, K.M., Njau, K.N., 2023. Assessing the impacts of land use and climate changes on river discharge towards Lake Victoria. Earth 4, 365–383. https://doi.org/10.3390/earth4020020.

Spurlock, F., Burow, K., Dubrovsky, N., 2000. Chlorofluorocarbon dating of herbicide-containing well waters in Fresno and Tulare counties, California. J. Environ. Qual. 29, 474–483. https://doi.org/10.2134/jeq2000.00472425002900020016x.

Stadler, S., Osenbrück, K., Knöller, K., Suckow, A., Sültenfuß, J., Oster, H., Himmelsbach, T., Hötzl, H., 2008. Understanding the origin and fate of nitrate in

groundwater of semi-arid environments. J. Arid Environ. 72 (10), 1830–1842. ISSN 0140-1963,. https://doi.org/10.1016/j.jaridenv.2008.06.003.

Strohmenger, L., Ackerer, P., Belfort, B., Pierret, M.C., 2022. Local and seasonal climate change and its influence on the hydrological cycle in a mountainous forested catchment, journal of hydrology, volume 610, 127914. ISSN 0022-1694. https://doi.org/10.1016/j.jhydrol.2022.127914.

Tweed, S., Celle-Jeanton, H., Cabot, L., Huneau, F., De Montety, V., Nicolau, N., Travi, Y., Babic, M., Aquilina, L., Vergnaud-Ayraud, V., Leblanc, M., 2018. Impact of irrigated agriculture on groundwater resources in a temperate humid region. Sci. Total Environ. 613–614, 1302–1316.

Uriostegui, S., Bibby, R., Esser, B., Clark, J., 2016. Quantifying annual groundwater recharge and storage in the Central Sierra Nevada using naturally-occurring 35 S: quantifying annual groundwater recharge and storage using 35 S. Hydrol. Process. 31. https://doi.org/10.1002/hyp.11112.

Van Der Min, J., 1945. Etude hydrogéologique des grands captages d'eau potable dans les coulées de lave des environs de Clermont-Fd.

Vittecoq, B., Gourcy, L., Baran, N. : Datation des eaux souterraines de Martinique par l'analyse conjointe des CFC, SF6 et tritium et relation avec les concentrations en nitrates et produits phytosanitaires. BRGM/RP-55844-FR, 50 pages, 29 illustrations, 2007.

Waibel, M.S., Gannett, M.W., Chang, H., Hulbe, C.L., 2013. Spatial variability of the response to climate change in regional groundwater systems – examples from simulations in the Deschutes Basin, Oregon. J. Hydrol. 486, 187–201. ISSN 0022-1694,. https://doi.org/10.1016/j.jhydrol.2013.01.019.

Warner, M.J., Weiss, R.F., 1985. Solubilities of chlorofluorocarbons 11 and 12 in water and seawater. Deep Sea Res. Part A. Oceanograp. Res. Papers 32 (12), 1485–1497. https://doi.org/10.1016/0198-0149(85)90099-8. ISSN 0198-0149.

Wigley, T. & Raper, S.: Interpretation of High Projections for Global-Mean Warming. Science (New York, N.Y.), vol. 293, 451–4, https://doi.org/10.1126/science.1061604, 2001.

Yokoyama, T., Takeuchi, S., 2009. Porosimetry of vesicular volcanic products by a water-expulsion method and the relationship of pore characteristics to permeability. Journal of geophysical research: solid. Earth 114.